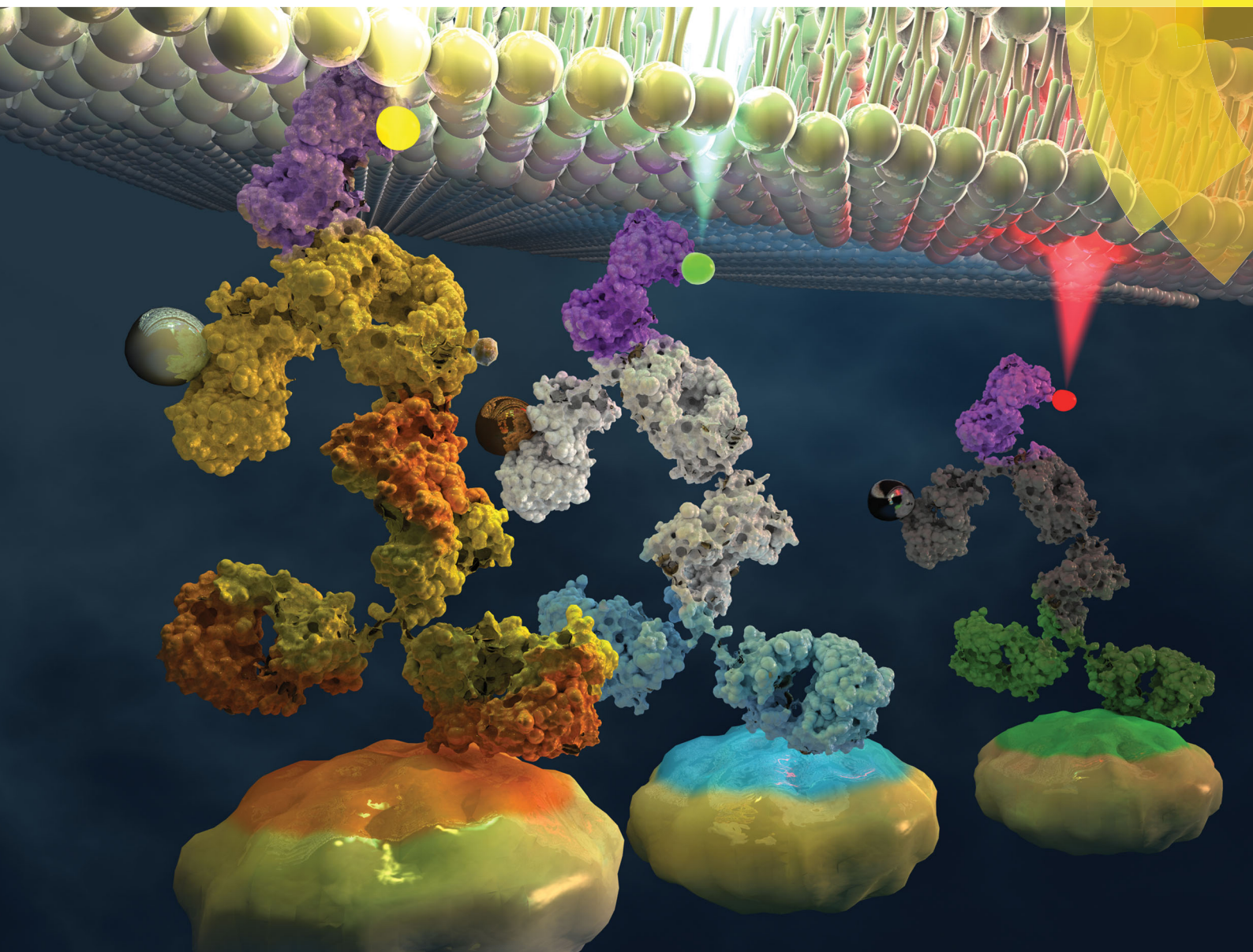


# Chem Soc Rev

Chemical Society Reviews

[rsc.li/chem-soc-rev](http://rsc.li/chem-soc-rev)



ISSN 0306-0012



TUTORIAL REVIEW

Dominic J. Hare *et al.*

A guide to integrating immunohistochemistry and chemical imaging



Cite this: *Chem. Soc. Rev.*, 2018, 47, 3770

## A guide to integrating immunohistochemistry and chemical imaging

David P. Bishop,  †<sup>ab</sup> Nerida Cole,  †<sup>abc</sup> Tracy Zhang,<sup>b</sup> Philip A. Doble <sup>b</sup> and Dominic J. Hare  \*<sup>abd</sup>

Chemical imaging provides new insight into the fundamental atomic, molecular, and biochemical composition of tissue and how they are interrelated in normal physiology. Visualising and quantifying products of pathogenic reactions long before structural changes become apparent also adds a new dimension to understanding disease pathogenesis. While chemical imaging in isolation is somewhat limited by the nature of information it can provide (e.g. peptides, metals, lipids, or functional groups), integrating immunohistochemistry allows simultaneous, targeted imaging of biomolecules while also mapping tissue composition. Together, this approach can provide invaluable information on the inner workings of the cell and the molecular basis of diseases.

Received 24th January 2018

DOI: 10.1039/c7cs00610a

[rsc.li/chem-soc-rev](http://rsc.li/chem-soc-rev)

### Key learning points

- (1) Chemical imaging must be redefined to encompass all analytical techniques that can spatially map the chemical composition of a sample.
- (2) Immunohistochemistry has many applications in chemical imaging, from co-localising individual proteins with chemical components to multiplexed experiments for profiling biochemical pathways and cell hierarchies.
- (3) The significance of an immunohistochemistry and chemical imaging approach is not necessarily based in technology, but how it is applied to answer a primary research question.
- (4) Immunostaining may inadvertently perturb the native biochemistry of the system being imaged, and the effects of each potentially confounding step should be considered when validating a method.
- (5) Combining immunohistochemistry with novel applications of chemical imaging presents new opportunities and technical challenges that should be considered research priorities to allow further growth in the field.

## 1. Introduction

The complexity of a biological system is reflected by the dynamic microchemical environment found within cells and tissues. Imaging technology has advanced to a point where specific biochemicals can be targeted and visualised, potentially in real time. Traditional anatomical pathology, for which visualising microstructure was once the primary outcome, has greatly benefited from advances in analytical technology and

their application to chemical imaging. Biologists now have a range of chemical imaging tools at their disposal that complement, and in some cases even supplant, conventional methods for spatially profiling the structure and biochemical makeup of cells, organs, and even whole organisms.

Histology and histochemistry are the standard approaches for visually assessing gross tissue morphology, cell type, subcellular structure, and the presence of endogenous chemicals that react to form coloured compounds with certain dyes and stains. While having an important place in both analytical biochemistry and diagnostics, these methods are primarily qualitative and have limited specificity at the molecular level. Many chemical components of biological systems fall outside the scope of traditional histochemistry and have necessitated the development of alternative approaches to reconstruct their spatial distribution. Simply identifying a biomolecule presents only a partial picture; visualising spatial distribution and associating it with structural or other biochemical features is crucial to fully understand involvement in a defined biological mechanism or relevance to disease.

<sup>a</sup> Elemental Bio-imaging Facility, University of Technology Sydney, Broadway, New South Wales, Australia

<sup>b</sup> Atomic Pathology Laboratory, The Florey Institute of Neuroscience and Mental Health, The University of Melbourne, 30 Royal Parade, Parkville, Victoria 3052, Australia. E-mail: dominic.hare@florey.edu.au; Tel: +61 3 9035 9549

<sup>c</sup> ARC Training Centre in Biodevices, Faculty of Science, Engineering and Technology, Swinburne University of Technology, Hawthorn, Victoria, Australia

<sup>d</sup> Department of Pathology, The University of Melbourne, Parkville, Victoria, Australia

† Contributed equally.



In the latter case, changes to the chemical properties and compartmentalisation of one or more disease-associated species often precede the appearance of cytopathology. Pathology may manifest from altered concentrations or chemical modifications that impart toxicity either independently or *via* aberrant interactions with other biological components, though simple redistribution of a biochemical without overt changes to chemical state or structure can also precipitate systemic dysfunction. Identifying when, and most importantly where, normal physiological conditions are disturbed is crucial for elucidating the molecular basis of disease. Accurately measuring the degree of change and where it occurs opens new avenues of investigation for targeted therapies and biomarker discovery.

The use of antibody labelling with a chemical marker was first described with fluorescent  $\beta$ -anthyryl-carbamide conjugated to anti-pneumococcus in 1941.<sup>1</sup> Biomolecules that were

previously undetectable using histochemical staining and light microscopy suddenly became 'visible'. Three-quarters of a century later, novel uses of technology (some by design, others through creative repurposing) and innovations across all sub-disciplines of chemistry have made available a diverse chemical imaging toolbox, spanning whole organs to single molecules and atoms.

Immunohistochemistry (IHC) has now become routine, although experimental protocols, reagents, detection techniques, and image analysis methods are constantly extending upon what information can be extracted. However, aside from a handful of clinically-approved protocols and the gradual uptake of automation outside high-throughput laboratories, it is also a somewhat imprecise science. Sample preparation requires substantial handling, chemical treatment and, when developing new assays, a degree of trial-and-error. When properly executed,



**David P. Bishop**

*Center for Duchenne Muscular Dystrophy (CDMD) working with Dr Jonathan Wanagat developing new methods for visualising disease biochemistry.*

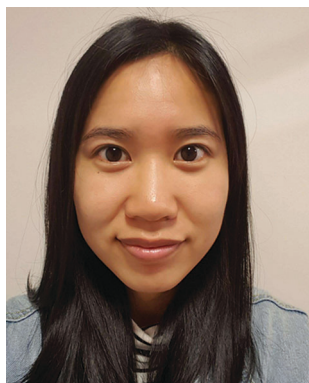
*David Bishop completed his BSc with 1st class Honours and PhD in Chemistry at the University of Technology Sydney. He is a current recipient of the Australian Research Council's Discovery Early Career Researcher Award, and his Fellowship is examining the translational utility of immunohistochemistry and chemical imaging in cell biology. He is a former Fullbright Scholar, spending part of 2016 at the University of California, Los Angeles (UCLA)*



**Nerida Cole**

*her breadth of knowledge across all facets of contemporary research are being used to accelerate translation of new discoveries to real-world solutions.*

*Nerida Cole received a BSc (Hons, 1st class) in Chemistry and MSc in Biochemistry from the University of Sydney, prior to completing a PhD in Optometry and Veterinary Science from the University of New South Wales. She has worked in research, teaching and research administration roles, and spent substantial time working on commercial research projects centred on the host-response to implanted biodevices. Now part of the Swinburne University of Technol-*



**Tracy Zhang**

*Tracy Zhang completed her BSc with 1st class Honours in 2017 at the Florey Institute of Neuroscience and Mental Health and The University of Melbourne in Behavioural Neuroscience, and was recently awarded a Parkinson's Victoria PhD scholarship to study the effects of brain iron over-exposure throughout lifespan at the Florey with Drs Dominic Hare, Emma Burrow and Scott Kolbe, using a range of in and ex vivo chemical imaging techniques.*



**Philip A. Doble**

*imaging tool for biologists and medical researchers, as well as the translation of advanced analytical chemistry technology into clinical research.*

*Philip Doble is Professor of Analytical Chemistry at the University of Technology Sydney and head of the Elemental Bio-imaging Facility. He completed his PhD in Chemistry in 1998 at the University of Tasmania studying the separation and detection of anions using capillary electrophoresis. Philip's main research interests involve the further development of laser ablation-inductively coupled plasma-mass spectrometry as an*



contemporary IHC is enormously powerful for analytical biochemistry; be it as a cell-specific marker for cytometry or probe sensitive only to the subtlest disease-associated chemical change occurring from single point genetic mutations. Coupling IHC with chemical imaging, in all its forms, expands the scope even further—now direct associations between antibody targets and other biological components can be made in single-origin samples. That being said, integrating IHC with chemical imaging is not trivial—considerable planning and preparation, paired with a good understanding of the fundamental principles that underpin both IHC and chemical imaging as separate disciplines is a necessity.

In this Tutorial Review we provide a guide for designing IHC imaging experiments that capitalise on the latest developments in chemical imaging using analytical spectroscopy and mass spectrometry. Integrated IHC and chemical imaging as a research tool falls into two categories with substantial overlap in terms of possible applications: (i) routine IHC protocols are applied in sequence or in parallel with chemical imaging for interrogating spatial associations and relationships between labelled antibodies and endogenous chemicals; and (ii) novel applications of IHC with diverse and exotic chemical reporters that extend beyond the capabilities of routine methods. We summarise the imaging technology available with a focus on the abilities and shortcomings intrinsic to each. We then discuss where sample preparation steps both align with and deviate from standard conventions for IHC, and how the necessary steps to prepare samples for IHC may impact endogenous chemicals of interest. Using the lessons learned from traditional IHC and the common chemical imaging methods employed, we outline how future validation studies should be designed for potential clinical translation. Finally, we examine a selection of novel examples of IHC-chemical imaging, highlighting the achievements that have been made, outline how specific research

questions are driving method development, and speculate on where the future potential of IHC-chemical imaging lies.

## 2. Redefining chemical imaging

The current definition of chemical imaging describes the use of spectroscopy to measure unique interactions between photons and matter in two, three, and occasionally four dimensions, though the emergence of imaging mass spectrometry (MS) in recent years justifies extension to include direct spatial profiling of chemical composition. This expanded definition shifts the focus to the shared ability of spectroscopy and spectrometry to collect multiple spectra reflecting specific chemical features present in a defined area, and to use this information to construct spatial measures of chemical distribution. This broader description of chemical imaging, when used in sequence and combined with IHC, emphasises that nearly every class of biomolecule is amenable to spatial analysis at resolutions extending from the mesoscale into the subcellular domain, depending on the method used. Rather than present an in-depth discussion of technologies available, we have summarised key features and considerations in the context of IHC-chemical imaging in Table 1 and direct the reader to key technical reviews and texts.

In most cases, combining IHC and chemical imaging does not necessarily supersede histochemistry; rather, it offers an opportunity to gather more detailed information about the presence, quantity, and chemical state of specific biomolecules. Each chemical imaging technique normally excels at one particular task, such as how Fourier-transform infrared (FTIR) and Raman spectroscopy can plot spectroscopic qualities of the predominant chemical environment while mass spectrometry imaging (MSI) uses a more targeted approach to isolate and map specific chemicals by mass. While investigation of a specific target may be optimally achieved with single imaging technique, the true power is in spatial profiling of multiple chemicals and using this data to decipher the complex interplay occurring between them. The utility of chemical imaging in biology is further enhanced by the capacity to simultaneously measure and spatially associate biomolecules identified with exogenous tags and unlabelled chemical species.

## 3. A beginner's guide to immunohistochemistry for chemical imaging

Antibodies are glycoproteins with a specific affinity to a portion of a target biomolecule, known as an antigen. The antigen-binding site, or paratope, of an antibody is sensitive to the epitope of the antigen, which may be as small as a specific amino acid sequence (linear epitopes) or as large as part of the antigen tertiary structure (conformational epitopes). Antibodies are part of an organism's innate immune response and can be produced with specificity for nearly all biomolecules, including misfolded or mutated variants involved in specific disease states. However, even the most robustly-validated and clinical-approved



**Dominic J. Hare**

*Dominic Hare completed a BSc in Applied Chemistry with 1st class Honours and a PhD in Chemistry at the University of Technology Sydney, under the supervision of Prof. Philip Doble. He was a co-founder of the Elemental Bio-imaging Facility, before relocating to the Florey Institute of Neuroscience and Mental Health at The University of Melbourne, where he currently heads the Atomic Pathology Laboratory. In 2016 he was awarded a prestigious*

*National Health and Medical Research Council Career Development Fellowship to establish a research program probing the role of iron as a possible causative feature of Parkinson's disease. He is a Fellow of the Royal Society of Chemistry and Advisory Board member of Metallomics.*



**Table 1** Summary of main technical features, capabilities and limitations of chemical imaging techniques compatible with IHC (charge-coupled device, CCD; focal plane array, FPA; Fourier-transform infrared, FTIR; laser ablation-inductively coupled plasma-mass spectrometry, LA-ICP-MS; laser induced breakdown spectroscopy, LIBS; secondary ion mass spectrometry, SIMS; surface-enhanced Raman spectroscopy, SERS; time-of-flight, TOF)

| Spectroscopic detection                  |  |  |                                |   |  |   |
|--|--|--|--------------------------------|---|--|---|
|  | Analyte type   | Target biochemicals and markers  | Typical image resolution range | Advantages  | Limitations  | Key technical references  |
| Light microscopy                         | <ul style="list-style-type: none"> <li>Chromogenic dyes and stains</li> <li>Enzyme-catalysed chromogens</li> </ul> | <ul style="list-style-type: none"> <li>Structural/organelle-specific markers</li> <li>Dye-specific substrates (proteins, carbohydrates, nucleic acids, etc.)</li> <li>Chromogenic substrate-tagged antibodies</li> </ul> | To 200–250 nm                  | <ul style="list-style-type: none"> <li>Rapid staining</li> <li>Digital image capture</li> <li>Wide image resolution range</li> <li>Capacity for high volume staining and image capture</li> <li>Automation</li> <li>Well suited to archived samples on standard glass mounts</li> </ul>                                   | <ul style="list-style-type: none"> <li>Diffraction limited</li> <li>Relatively non-specific (dyes and stains)</li> <li>Inconsistent staining and variable contrast</li> <li>Quantitative analysis limited by observational scoring and interobserver bias</li> </ul>   | Thorn <sup>2</sup>  |
| Epifluorescence/confocal microscopy      | <ul style="list-style-type: none"> <li>Fluorophores</li> </ul>   | <ul style="list-style-type: none"> <li>Fluorophore-tagged antibodies</li> <li>Structural/organelle-specific markers</li> <li>Small molecules</li> <li>Fluorescent proteins</li> </ul>                                    | To 200–250 nm                  | <ul style="list-style-type: none"> <li>High specificity</li> <li>Diverse range of targets</li> <li>Live cell imaging</li> <li>Three-dimensional imaging (confocal)</li> <li>Potential for quantitative analysis</li> </ul>  | <ul style="list-style-type: none"> <li>Diffraction limited</li> <li>Autofluorescence interference</li> <li>Photobleaching</li> <li>Phototoxicity (live-cell imaging)</li> <li>Spectral overlap limits multiplexing to &lt; 10 analytes</li> </ul>  | Kubitscheck; <sup>3</sup> Thorn <sup>2</sup>                                    |
| Super-resolution microscopy              | <ul style="list-style-type: none"> <li>Fluorophores</li> </ul>   | <ul style="list-style-type: none"> <li>Fluorophore-tagged antibodies</li> <li>Structural/organelle-specific markers</li> <li>Small molecules</li> <li>Fluorescent proteins</li> </ul>                                    | 250–20 nm                      | <ul style="list-style-type: none"> <li>Nanoscale imaging</li> <li>High specificity</li> <li>Diverse range of targets</li> <li>Live cell imaging</li> <li>Fast confocal imaging</li> <li>Reduced phototoxicity</li> </ul>  | <ul style="list-style-type: none"> <li>Requires bright fluorophores</li> <li>Emerging technology with limited turnkey options</li> <li>Large field of views restricted by scanning speeds and high resolution</li> <li>Resolution and multiplexing limited for large antigen-1°–2°-antibody complexes</li> </ul> | Kubitscheck; <sup>3</sup> Thorn; <sup>2</sup> Vogler <i>et al.</i> <sup>4</sup> |
| Electron microscopy (EM)                 | <ul style="list-style-type: none"> <li>Structural components</li> <li>Nanoparticles</li> </ul>                     | <ul style="list-style-type: none"> <li>Heavy-metal contrast-enhanced ultrastructure</li> <li>Gold nanoparticle-tagged antibodies</li> </ul>  | 200 nm–50 pm                   | <ul style="list-style-type: none"> <li>Molecular-level resolution</li> <li>Multiplexing possible with gold nanoparticle conjugates of differing diameters</li> <li>Simultaneous elemental analysis by energy-dispersive X-ray spectroscopy (EDX)</li> <li>Environmental scanning (ES)EM for hydrated specimens</li> </ul> | <ul style="list-style-type: none"> <li>Complex sample preparation and analysis</li> <li>Requires 50–100 nm sections</li> <li>Vacuum required for non-ESEM</li> <li>Potential radiation effects on hydrated samples in ESEM</li> <li>Specialised sample mounts</li> </ul>   | Fernandez-Leiro and Scheres <sup>5</sup>  |
| X-ray emission/fluorescence spectroscopy | <ul style="list-style-type: none"> <li>Structural components</li> <li>Elements</li> </ul>                          | <ul style="list-style-type: none"> <li>Ultrastructure</li> <li>Metal-labelled antibodies</li> </ul>  | 1 μm–10 nm                     | <ul style="list-style-type: none"> <li>Density and structural information from untreated samples</li> <li>High specificity and multiplexing using metal-labelled antibodies</li> </ul>  | <ul style="list-style-type: none"> <li>Requires synchrotron radiation for high resolution imaging</li> <li>Overlapping K-shell emission lines reduce sensitivity for many bioelements</li> </ul>   | McRae <i>et al.</i> <sup>6</sup> Pushie <i>et al.</i> <sup>7</sup>              |



Table 1 (continued)

| Spectroscopic detection                                |  |   |   |   |   |  |
|--|--|---|---|---|---|--|
| Analyte type   | Target biochemicals and markers  | Typical image resolution range  | Advantages  | Limitations   | Key technical references  |  |
| Infrared and vibrational spectroscopy                  | <ul style="list-style-type: none"> <li>Organic compounds</li> <li>Nano-particles (for SERS)</li> </ul> | <ul style="list-style-type: none"> <li>Proteins, carbohydrates, nucleic acids, <i>etc.</i></li> <li>Vibrational tagged antibodies (for Raman spectroscopy)</li> <li>Gold nanoparticle conjugated antibodies (for SERS)</li> </ul> | 10–4 $\mu\text{m}$ (FTIR); 1 $\mu\text{m}$ –400 nm (Raman)      | <ul style="list-style-type: none"> <li>Spatial mapping of element oxidation state</li> <li>No sample preparation when using cryostreams</li> <li>Potential for quantitative analysis</li> <li>Rapid and simultaneous collection of over 10 000 spectra using FPAs</li> <li>Live-cell imaging (Raman)</li> <li>Combined FTIR and Raman microscopes available</li> <li>Selection of specific wave-numbers increases sensitivity</li> <li>Quantitative volumetric imaging</li> </ul> | <ul style="list-style-type: none"> <li>Time-consuming spectral deconvolution for imaging</li> <li>Photoreduction and radiation-induced observer effects</li> <li>Specialised sample mounts</li> <li>Detection of functional groups only is relatively non-specific</li> <li>General low sensitivity</li> <li>Long spectral collection times</li> <li>Specialised sample mounts</li> </ul> | Vogler <i>et al.</i> <sup>4</sup>  |
| Atomic emission spectroscopy                           | <ul style="list-style-type: none"> <li>Elements</li> </ul>   | <ul style="list-style-type: none"> <li>Endogenous elements</li> <li>Metal-labelled antibodies</li> </ul>  | 200–10 $\mu\text{m}$  | <ul style="list-style-type: none"> <li>Simultaneous detection using CCD cameras</li> <li>Low-volume sampling with minimal sample damage</li> <li>Potential for quantitative analysis</li> <li>Simultaneous LIBS and Raman imaging using common laser source</li> </ul>  | <ul style="list-style-type: none"> <li>Few reported applications in bioimaging</li> <li>Low sensitivity for many endogenous elements</li> <li>Low spatial resolution</li> </ul>   | Kaiser <i>et al.</i> <sup>8</sup>  |
| Spectrometric detection<br>Molecular mass spectrometry | <ul style="list-style-type: none"> <li>Organic compounds</li> </ul>                                    | <ul style="list-style-type: none"> <li>Proteins, carbohydrates, lipids, <i>etc.</i></li> <li>Metabolites and small molecules</li> <li>Photocleavable mass tags</li> </ul>   | 200–1 $\mu\text{m}$   | <ul style="list-style-type: none"> <li>Direct detection of high-abundance species</li> <li>IHC and on-tissue for antigen-specific <math>F_{\text{ab}}</math> and V fragments</li> <li>Selective and sensitive photocleavable mass tags suitable for highly-multiplexed imaging</li> <li>Potential for quantitative analysis</li> <li>Wide range of application-specific ambient ionisation sources</li> </ul>   | <ul style="list-style-type: none"> <li>Limited sensitivity for high mass compounds and low abundance biomolecules</li> <li>Low spatial resolution</li> <li>Specialised sample mounts</li> </ul>   | Bodzon-Kulakowska and Suder; <sup>9</sup> Buchberger <i>et al.</i> <sup>10</sup> |
| Elemental mass spectrometry                            | <ul style="list-style-type: none"> <li>Elements</li> </ul>   | <ul style="list-style-type: none"> <li>Endogenous elements</li> <li>Metal-labelled antibodies</li> <li>Small molecules (for SIMS)</li> </ul>  | 200–1 $\mu\text{m}$ (LA-ICP-MS); 1 $\mu\text{m}$ –100 nm (SIMS) | <ul style="list-style-type: none"> <li>High sensitivity</li> <li>Simultaneous detection (for TOF-MS and SIMS)</li> <li>Potential for quantitative analysis</li> <li>Commercial systems for highly-multiplexed imaging (MaxPar<sup>®</sup> reagents and LA-CyTOF-MS)</li> </ul>  | <ul style="list-style-type: none"> <li>Substantial matrix effects (for ICP-MS)</li> <li>Low spatial resolution (for ICP-MS)</li> </ul>  | McRae <i>et al.</i> <sup>6</sup>   |

IHC assays are prone to analytical error and interference, and the number of research-only applications dwarfs those that have been approved for clinical use. Prior to explicit guidelines for

IHC analytical validation issued by the US College of American Pathologists (CAP) Pathology and Laboratory Quality Center in 2014 (discussed in detail in Section 3.4),<sup>11</sup> clinical pathology



laboratories had no set instructions to follow, and instead either replicated prior examples of validated and Food and Drug Administration (FDA)-approved predictive immunoassays (such as the oncogene-product human epidermal growth factor 2 [HER2]), or developed internal method validation protocols.

Considering that IHC-chemical imaging is still in relative infancy, now is a critical time to establish consensus-driven guidelines for method development and eventual clinical translation. Instituting such standards cannot be the responsibility of one laboratory or research group, though we can identify key considerations in designing chemical imaging experiments that employ antigen-specific detection for both immediate research use, and as parameters for future multi-site concordance studies. It is also important to recognise that, in a rapidly growing field, new confounding factors are constantly being identified, and designing future experiments should encompass these as they are reported.

At this point it is also important to make a clear distinction in the nomenclature used throughout this Tutorial Review: when referring to an analyte, we are describing the species that is directly detected using chemical imaging, whereas antigen is used to describe the associated biomolecule (Fig. 1).

The class of analyte suitable for IHC-chemical imaging is limited only by what can form a stable and specific association with either the primary or secondary antibody. Traditional IHC relies on spectroscopic properties of the analyte, such as propensity to form a coloured precipitate with specific stains or fluoresce when excited. Manipulating photon-matter interactions and improving how they are detected drives development of new technology. Fluorescence microscopy can therefore be considered as both routine—it is one of the most widely used laboratory techniques in the world—and intersecting the cutting-edge of physics, chemistry and biology. Recent technical advances, such as overcoming the light diffraction limit to allow super-resolution microscopy certainly offer unique opportunities, though 'routine' fluorescence microscopy is still central to many IHC-chemical imaging applications. This highlights a key learning point: the significance of an imaging approach is not necessarily based in technology, but how it is applied to answer a primary research question. The development of a new analyte, its integration into an existing IHC protocol, and use in aiding visualisation of the surrounding microchemical environment is as important as emergence of new imaging techniques. In this Tutorial Review, we focus on selecting (or developing) the analyte rather than imaging technique, acknowledging that certain analyte classes are applicable to multiple analytical methods.

As most protocols involve labelling an antibody with an analyte prior to incubation with a sample, standard protocols for IHC are generally applicable. Depending on the analyte, an IHC-chemical imaging experiment may use primary antibodies pre-labelled with a chemical reporter, or apply labelled secondary antibodies as an amplification step (Fig. 2). Both approaches have intrinsic advantages and limitations related to the choice of analyte and imaging technique. In this section, we provide a guide to developing an IHC-chemical imaging experiment, emphasising the importance of good experimental design based on the principles of analytical method validation.

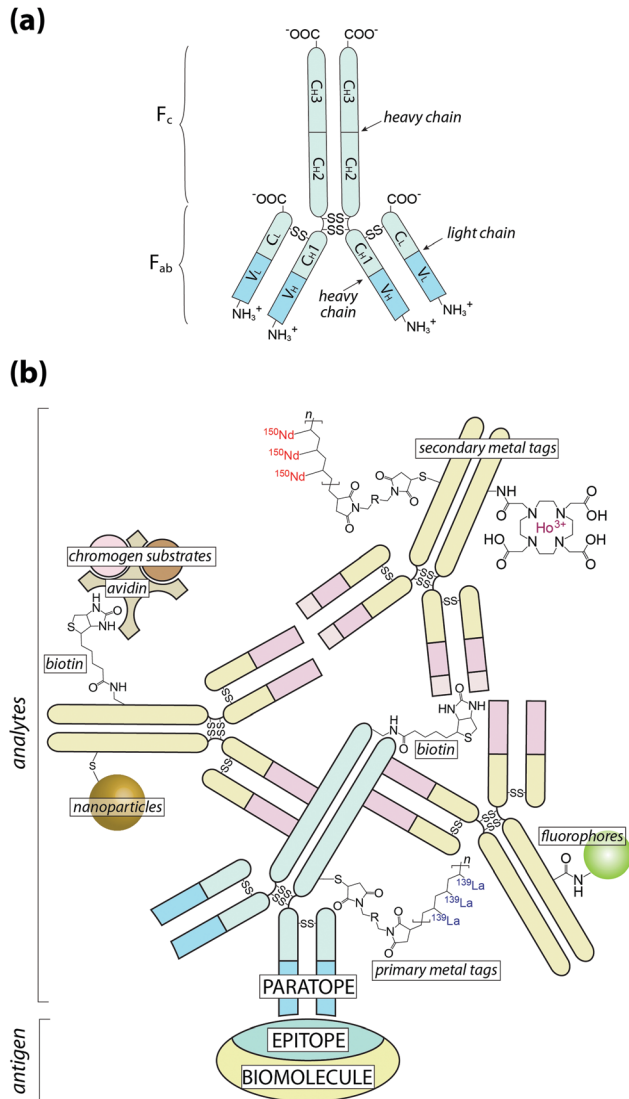


**Fig. 1** Schematic of antigen-antibody binding for detecting biomolecules. (a) Antibodies are large glycoprotein immunoglobulins with a 'Y'-shaped monomeric structure. The two ~50 kDa heavy chains consists of three constant domains (C<sub>H1</sub>–3) and a N-terminus variable domain (V<sub>H</sub>) that forms one half of the antigen-binding site. The two light chains (~25 kDa) contain a constant domain (C<sub>L</sub>) at the C-terminus and a corresponding variable domain (V<sub>L</sub>) to complete the antigen-binding paratope. Interchain disulfide bonds link the heavy and light chains within the constant domains, with two additional disulfide bridges at the hinge region between C<sub>H1</sub> and C<sub>H2</sub>. The Fab region contains the paratope, whereas the F<sub>c</sub> region is the site of secondary antibody binding. (b) Primary antibodies recognise specific amino acid sequences or structural features of the antigen, referred to as the epitope, at 1:1 stoichiometry. Signal amplification is typically achieved by secondary antibodies labelled with a fluorophore or chromogen, though metal tags have specific applications. Multiple binding sites in the F<sub>c</sub> region increases the number of chemical analytes that can be associated with a single antigen (see Fig. 2).

### 3.1 Designing an IHC-chemical imaging experiment

The first question an analyst should ask when embarking on experiments that integrate IHC with chemical imaging is: can the intended outcome provide information not currently achievable with existing protocols and technology? Developing a method



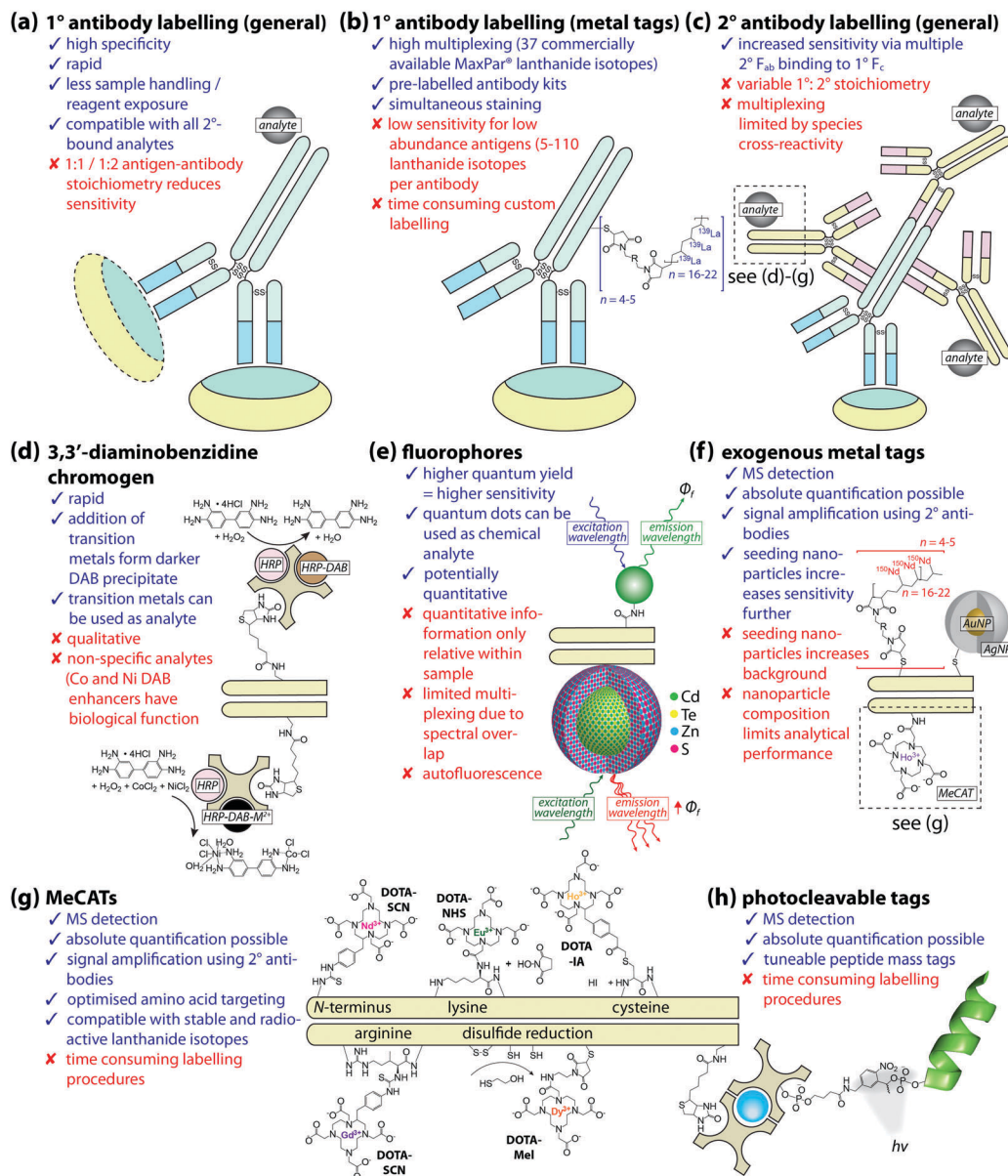


**Fig. 2** Antibodies and analytes for IHC-chemical imaging. (a) Primary (1°) antibodies provide the highest specificity and greatest potential for multiplexing using unique chemical reporters (such as isotopically-enriched lanthanides); (b), though have lower sensitivity. (c) Secondary (2°) antibodies raised against the primary host organism are therefore used to amplify signal and improve detection limits, coming with their own limitations. (d) Light microscopy employs chromogens, normally linked to the 2° IgG via a biotin-streptavidin complex with a peroxidase (shown here as horseradish peroxidase, or HRP) substrate for 3,3'-diaminobenzidine (DAB) oxidation. Addition of divalent metal ions (e.g. Ni<sup>2+</sup>, Co<sup>2+</sup>) forms a darker precipitate, and while these could be used as a proxy for imaging by LA-ICP-MS, caution should be taken due to potential interference from physiological sources. (e) Fluorophores use an excitation source to induce emission of Stokes-shifted photons with brightness proportional to the product of the fluorophore quantum yield ( $\phi_f$ ) and extinction coefficient. Quantum dots are photon-emitting nanomaterials with cores comprised of group II–VI, group III–V, or group IV–VI binary compounds and zinc sulfide shells that produce stable, bright, and narrow emission spectra which can be tuned by manipulating particle size. Quantum dots can be conjugated to antibodies via several methods, most commonly using –COOH, –NH<sub>2</sub> and –SH functional groups on the particle surface to crosslink with amino acids. In addition to superior  $\phi_f$ , near-infrared properties of quantum dots can be exploited with IR imaging, and the exogenous metal/metalloid composition with atomic spectrometry. (f) Gold and silver nanoparticles (Au/Ag NP) are particularly useful in MS imaging for amplifying signal attributable to low-abundance antigens, or as a substrate for SERS; while MeCATs use 1,4,7,10-tetraazacyclododecane-1,4,7,10-tetraacetic acid (DOTA) macrocycles to chelate lanthanide ions, including radionuclides. (g) Addition of prosthetic reactive groups permits selective binding of the DOTA chelate to specific amino acid residues on the IgG carrier (isothiocyanate, SCN; *N*-hydroxysuccinimide, NHS; maleimide, Mel; iodoacetamide, IA). (h) Photocleavable tags are also used in MS imaging, and typically consist of a peptide of known mass and structure linked to a photosensitive moiety and biotin-avidin complex, represented here with an avidin-coated glass bead.

using a novel chemical analyte that produces a similar result to that which could be obtained using traditional methods may be

of interest to a subset of researchers, though its potential impact within the wider field of anatomical pathology will be limited.





Where it is clear that traditional IHC approaches are insufficient to answer the question at hand and that chemical imaging offers capabilities that overcome such limitations, the next step is to identify what properties of the sample in question are subject to analysis. These include, but are not limited to, quantifying the amount of endogenous chemicals present, spatial assessment of how multiple antigens and biochemicals interact, high-resolution imaging of subcellular compartmentalisation, or even providing complementary information for traditional IHC methods. Here we provide here a guide based on known quantities that various chemical imaging methods can inform. The reader should not consider this list exhaustive as the discipline is rapidly evolving, and the emergence of new technologies will see the scope of IHC-chemical imaging broaden.

**3.1.1 Analytical sensitivity.** Use of the terms sensitivity (the smallest amount of analyte detectable) and specificity (the confidence that the measured signal is representative of only the analyte) in an analytical context should not be confused with diagnostic sensitivity and specificity of IHC, which refers to the ability of an assay to reliably detect a specific disease-associated antigen. As such, a scenario can exist where an IHC assay has high diagnostic sensitivity and specificity while the antigen in question is present at high levels, and only in a certain disease state.

Immunohistochemical detection of an antigen can be divided into two categories: (i) direct detection, where the primary antibody is conjugated to a suitable analyte in the  $F_c$  domain; or (ii) indirect detection, where an immunoglobulin (typically IgG) raised against the primary host species (*e.g.* rabbit anti-mouse IgG for a murine-derived primary antibody) with a conjugated analyte is introduced. Direct detection requires fewer sample processing steps and has a high capacity for multiplexing by eliminating species cross-reactivity of secondary antibodies, though in the majority of cases antibody-to-antigen stoichiometry is 1 : 1 which can limit sensitivity relative to indirect detection. The signal intensity attributable to the analyte is proportional to its concentration—which is technically an indirect measure of total antigen recognition by the primary antibody, though we use terms specific to IHC protocols in this Tutorial Review—and as multiple secondary antibodies can bind to the  $F_c$  region of a primary immunoglobulin, signal amplification is achieved by increasing the number of analytes associated with a single antigen.

Sensitivity is also determined by the detection technique. Spectroscopic chemical imaging requires the ability to detect and spatially resolve subtle changes in energy resulting from interactions between photons and matter, while mass spectrometry-based imaging depends on efficient physical transfer, separation, and detection of material directly removed from the sample surface. For a technique such as matrix assisted laser desorption/ionisation (MALDI) MS, this can be as little as 1–10 attomoles of total material per pulse (depending on laser and matrix conditions),<sup>12</sup> within which the total analyte may be present at levels several orders of magnitude lower.

The amount of detectable signal that can be attributed to a defined area determines both the sensitivity and achievable spatial resolution (see Section 3.1.3) of an imaging technique. Technical limits such as focal point, laser pulse diameter and

the dynamic range of the detector are nominally fixed, making control of variables in sample preparation and IHC protocols the major determinant of analytical sensitivity. A successful IHC protocol applied to chemical imaging should demonstrate reproducible measurements of analyte areal density with high signal-to-noise.

Equal attention should also be given to the practical detection limits for endogenous chemicals of interest. Factors to consider include whether the dynamic range of the detector is compatible with the different concentration ranges of the analytes and associated biochemicals, if further chemical derivatisation is necessary, and whether an additional mode of detection should be used in sequence. It is not uncommon for individual factors affecting sensitivity of either the analyte or endogenous chemicals to impose a compromise in imaging parameters used.

**3.1.2 Antibody specificity.** Specificity refers to the ability of the primary antibody to bind exclusively to the epitope of the antigen against which it was raised. Monoclonal antibodies are more specific than polyclonal variants as they recognise a single epitope on an individual antigen with the same affinity (known as monovalence). The trade-off is that they are more expensive to produce and are less sensitive, requiring substantial signal amplification for most detection techniques. Polyclonal antibodies recognise several epitopes on one or more antigens with differing degrees of affinity (polyvalence). The increased binding enhances sensitivity, though variable antibody–antigen stoichiometry and non-specific binding to equivalent epitope structures in other biomolecules introduces a degree of ambiguity for experiments where relative comparisons are made. Specificity is further complicated by inconsistencies in binding efficiencies between suppliers and the clones used to produce antibodies, and this is an important factor to consider when validating an IHC-chemical imaging protocol (see Section 3.3).

**3.1.3 Image resolution.** Fluorescence microscopy by far offers the highest practical spatial resolution, and the breakthrough of the 200 nm diffraction limit achieved by super resolution microscopy allows images approaching the low nanometre scale. Contemporary electron and scanning-probe microscopy systems are capable of resolving structural features in the picometre range, though it could be argued that imaging antibody–antigen complexes at such a resolution exceeds the requirements of most IHC experiments—atomic force microscopy was used to determine that a single antibody is approximately 20 nm in diameter.<sup>13</sup> Particle and X-ray-induced atomic emission spectroscopy are capable of producing sub-micron resolution images, and simultaneously spatially profile physical properties of a sample that can be related to cell structures.

With the exception of secondary-ion mass spectrometry (SIMS), MS imaging techniques are typically limited to meso-scale ( $> 1 \mu\text{m}$ ) resolution. This is primarily due to the same determinants of sensitivity, and resolution will improve as MS technology does.

## 3.2 Developing an IHC-chemical imaging experiment

The next question to be addressed when designing an experiment is: how can the desired outcome be met? This requires an



understanding of the variables that influence analytical validity and knowledge of the strengths and limitations of the imaging technique used. There is no universal protocol or checklist to follow for integrating IHC with chemical imaging—antibodies and biological systems are a far cry from the standard reference materials an analytical chemist would typically use to develop and validate a new method. Acknowledging that combined IHC and chemical imaging is an emerging field where potential measures and experimental outcomes are still being actively developed, we provide a general guide that can be adapted to suit the experiment to be performed.

### 3.2.1 Considerations when preparing samples for IHC.

Biological samples are a heterogeneous mixture of elements, inorganic and organic small molecules, peptides, proteins, nucleic acids, lipids, and carbohydrates. Cell structures have unique chemical environments resulting from how these components are structurally arranged and their relative concentrations. Any IHC experiment requires some form of sample pre-treatment. Fixation preserves cell structure and immobilises biomolecules—a sample will degrade if metabolic processes continue *ex vivo*. Antigen retrieval is often needed to ‘undo’ the chemical and physical modifications that fix proteins in place. Permeabilising cell membranes opens cellular compartments to large immunoglobulins while also allowing labile species to diffuse out. Long-term storage requires complete dehydration and infiltration with paraffin to retain cell morphology.

Each step exerts some influence on the microchemical environment, dependent on preparation method and the class of chemical affected (Fig. 3). A true depiction of an undisturbed biological system is inherently unobtainable; even live-cell imaging is subject to an ‘observer effect’, a concept that acknowledges chemical alterations can result from the imaging technique itself.<sup>14</sup> As such, there is no ‘standard’ of a completely undisturbed system against which an image can be compared, and the few studies that have specifically measured chemical alterations resulting from sample preparation indicate the effects are wide-ranging and cover every class of biochemical. When developing an IHC protocol intended to assess spatial relationships between antibody-bound antigens and native species, the aim should be to both minimise *ex vivo* perturbations to natural chemical distribution and, while recognising that some degree of modification is unavoidable, ensure all samples undergo identical preparation procedures.

Cryofixation is the least damaging form of sample preservation and is the preferred method for the majority of chemical imaging techniques, though it is also the most technically challenging. Rapid uniform cryogenic freezing vitrifies a sample, transforming liquid H<sub>2</sub>O into molecularly-disordered amorphous ice. By preventing H<sub>2</sub>O molecules from assembling into a hexagonal lattice structure, damage to cell morphology resulting from ice crystal growth is minimised. Cryoprotectants including polyethylene glycol and disaccharides can also be added to reduce crystal formation. Water is then removed by either addition of cooled organic solvents (freeze-substitution) or sublimation *via* low pressure lyophilisation, after which IHC can be performed on resin-embedded sections at standard laboratory

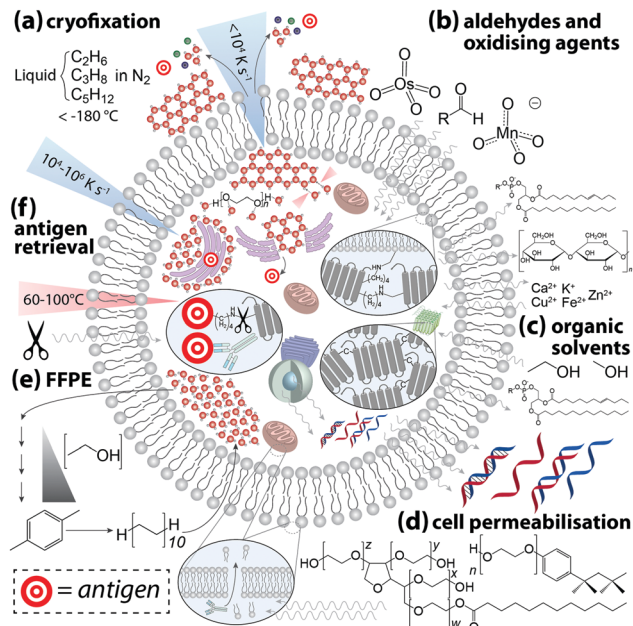


Fig. 3 Sample processing steps for IHC and associated effects on native cell biochemistry. (a) The aim of cryofixation is to cool the cell at a rate that prevents H<sub>2</sub>O molecules forming an ordered crystalline structure in favour of an amorphous glass-like disordered arrangement of supercooled H<sub>2</sub>O molecules that retains mechanical properties of a liquid. If the rate of cooling is too slow spontaneous nucleation and growth of ice crystals can rupture membranes, damaging cellular microstructures and causing both intra- (e.g. release of immature proteins from inside ribosomes on rough endoplasmic reticulum into the cytoplasm) and intercellular (e.g. interstitial exchange of molecules and ions through ruptured cell membranes as a result of changing concentration gradients) chemical redistribution. Cryoprotectants (e.g. polyethylene glycol) can hinder ice crystal formation by temporarily stabilising liquid H<sub>2</sub>O *via* hydrogen bonding. (b) Aldehydes and oxidising agents diffuse across the cell membrane and covalently crosslink lysine residues with an aliphatic bridge, disrupting tertiary protein structure while also anchoring proteins to cell membranes. Proteins, phospholipids and carbohydrates are partially lost to aldehyde fixation, and labile metals undergo two-way exchange. (c) Alcohols and organic solvents rapidly denature proteins to induce aggregation while simultaneously permeabilising membranes. This causes a loss of phospholipids and leaching of nucleic acids into the cytosol. (d) Non-ionic surfactants (e.g. polysorbate-20, Triton X-100) permeate bilipid membranes and allow antibodies to penetrate cells and organelles, which undoubtedly causes some degree of chemical redistribution. (e) Long-term archiving of biological samples at room temperature requires protein stabilisation, dehydration, and substitution of H<sub>2</sub>O with aliphatic hydrocarbons *via* formalin fixation and paraffin embedding (FFPE). (f) Fixation and preservation may mask the target epitope, thus heat or proteolytic (e.g. trypsin) cleavage of crosslinks, known as antigen retrieval, may be necessary to expose antigens to the antibody paratope.

conditions. Optimal cryofixation methods vary depending on sample type, and detailed protocols can be found in the book by Wolkers and Oldenhorf.<sup>15</sup> Excellent preservation of cell ultrastructure makes cryofixation particularly attractive for electron microscopy, and subsequent immunostaining with gold-nanoparticle conjugated antibodies has been used to demonstrate superior labelling efficiency of insoluble proteins compared to chemically-fixed samples.<sup>16</sup> Rapid freezing of whole tissue samples followed by cryosectioning and chemical fixation of cut tissue is an alternative approach for imaging techniques

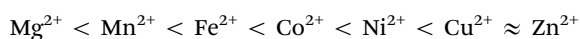


where damage to cell ultrastructure is beyond the practical image resolution obtained.

Aldehydes, oxidising agents, and organic solvents are the most commonly-used chemical fixatives. Aldehydes and oxidants forms covalent cross-links between amino acids, stabilising protein structure and anchoring proteins to cell membranes. Organic solvents denature proteins and induce the formation of insoluble aggregates. Fixation efficiency is determined by adequate penetration of a cell; therefore, exposure time, sample thickness, and temperature are variables that may produce inconsistencies. Organic solvents have the advantage of simultaneously permeabilising the cell, while aldehyde fixation is normally followed by immersion in a buffer containing a non-ionic surfactant. By removing lipids from the outer cell membrane antibodies are able to penetrate the cell, though removing such barriers allows soluble chemicals to diffuse beyond their native cellular compartment.

Hackett *et al.*<sup>17</sup> applied a multimodal imaging approach using both FTIR and PIXE imaging to assess effects of formalin fixation on the native microchemistry of neurological tissue. Using cryofixed and freeze-substituted tissue as a reference, FTIR spectra demonstrated marked decreases in vibrational intensities assigned to amides, olefinic carbon–hydrogen bonds, covalent carbon–oxygen bonds, and phosphates, indicating loss of proteins, carbohydrates, lipids, and lipid oxidation products. Even simple immersion in phosphate buffered saline had measurable effects on organic content. Hobro and Smith<sup>18</sup> capitalised on the ability of Raman spectroscopy to image live cells to evaluate the effects of immersion in aldehydes, organic solvents, and permeabilising surfactants. All reagents produced measurable changes in Raman spectra indicative of chemical redistribution and structural modification. This study is particularly informative as it not only demonstrates the differential effects of each reagent, but also how ambient conditions and order of chemical exposure can be optimised to preserve a specific class of biomolecule.

Unsurprisingly, both studies found that cytoplasmic proteins are particularly susceptible to leaching and redistribution. The same can also be said for labile and weakly-bound inorganics; quantitative elemental mapping of formalin-fixed brain tissue sections using PIXE showed near-total loss of intracellular potassium and reduction in chlorine. Conversely, calcium and the major biologically-relevant transition metals (iron, copper and zinc) all showed increased concentrations within cells. Similar observations were made by Chwiej *et al.*,<sup>19</sup> who used X-ray fluorescence spectroscopy to show differential influx and efflux of biologically-relevant elements in various areas of rat brain sections following formalin or paraformaldehyde fixation, with paraffin-embedded counterparts showing a marked decrease in nearly all measured elements. External contamination is clearly a point of consideration; when high-purity reagents are used, aldehyde fixation and sucrose cryoprotection resulted in loss of most biologically-relevant metals.<sup>20</sup> The degree of metal loss is not uniform, and species-specific effects can be attributed to variable affinities of metals to protein ligands, per the Irving–Williams series:<sup>21</sup>



Archived samples provide cost-effective access to a vast array of disease states and tissue types, though stability during long-term storage necessitates substantial chemical treatment. Samples are fixed in formalin over several hours, dehydrated and cleared in ethanol and xylene, then infiltrated with and embedded in paraffin for indefinite storage at room temperature. A comprehensive review of *ex vivo* modifications to proteins, nucleic acids and cell structure resulting from formalin-fixation and paraffin embedding (FFPE) protocols is detail in Bass *et al.*<sup>22</sup> Use of archived FFPE tissue introduces several sources of analytical uncertainty—initial fixation time, FFPE protocol and other pre-treatments such as decalcification are not typically recorded and likely vary between repositories. Immunoreactivity decreases over time, though antigen decay is not uniform,<sup>23</sup> meaning comparisons should only be made between samples of a similar age that underwent an identical FFPE protocol, and even then observations are empirical.

Finally, cross-linked proteins often mask an antigenic site and antigen retrieval may be necessary to expose sufficient numbers of epitopes prior to antibody incubation. The two most common methods used are: (i) heat-induced, where the sample is incubated in buffers containing surfactants and EDTA at high temperature and pressure; and (ii) protease-induced, where protein cross-links are enzymatically cleaved. Both approaches undoubtedly cause modifications to other biomolecules, and it is fitting that the authors of the first heat-induced antigen retrieval protocol commented on the need for standardisation in IHC, particularly regarding chemical fixation.<sup>24</sup> Over a quarter of a century later, many of the cautions raised have still not been addressed.

Chemical alterations to the sample during preparation for IHC are ultimately unavoidable. Therefore, steps taken should be sufficient to produce adequate (and equivalent) immunostaining using conditions that are both compatible with the antibody used and have minimal effects on the native biochemicals being analysed.

**3.2.2 Optimising antibody concentration.** Commercially-available antibodies ship with comprehensive datasheets, suggesting optimal experimental parameters based on the intended application, including IHC staining of frozen and FFPE sections, and detection method used (*e.g.* fluorescence, light or electron microscopy). Most datasheets provide suggested concentrations for routine optical microscopy. While recommended dilutions may not be optimal for the analyte or chemical imaging technique used, preparing samples in parallel for fluorescence or light microscopy provides a useful point of reference for further method development and quality control.

Non-specific binding below the ordinary threshold of detection for routine microscopy may cause significant interference when more sensitive chemical imaging modalities are used. Conversely, higher antibody concentrations may be necessary for detecting certain analytes. When a new antibody is being tested, a titration experiment should be performed specific to the detection method used where antibody concentration is the only variable. This is also the ideal point to prepare an isotype control, where the primary antibody is substituted with an



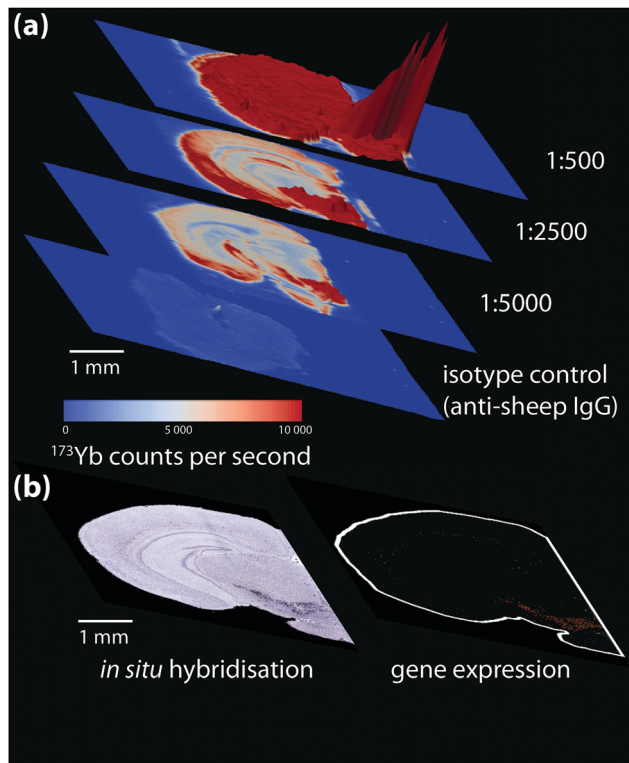


**Fig. 4** (a) Isotype control and titration experiment for a  $^{173}\text{Yb}$ -labelled sheep anti-mouse tyrosine hydroxylase (TH) primary antibody-stained coronal mouse brain section, imaged using LA-ICP-MS.  $^{173}\text{Yb}$ -labelled sheep IgG, which should have no specific reactivity to mouse tissue, shows a uniform pattern of non-specific binding slightly above background. Increasing antibody concentration increases background to a point where non-specific binding decreases signal-to-noise to a point that obscures antigen-specific analyte signal. (b) *In situ* hybridisation and gene expression maps from the Allen Brain Atlas<sup>25</sup> can be used as additional reference for wild-type protein distribution; here, sections taken at the same anatomical coordinates shows TH expression is mainly in the lower right quadrant of the brain hemisphere containing the basal ganglia formation.

otherwise-identical immunoglobulin raised against an antigen not present in the sample to determine levels of non-specific binding (Fig. 4). These should also be conducted in parallel with conventional immunohistochemical detection by optical microscopy.

**3.2.3 Multiplexing.** Several antigens can be visualised in a single multiplexed IHC experiment. Multiplexed IHC ranges from routine colocalisation studies of three analytes to high-powered computational image analysis of over two dozen labelled proteins. Multiplexing is highly relevant to chemical imaging as it both demonstrates the capabilities of non-traditional IHC imaging methods, and it provides new opportunities for multivariate profiling of complex molecular pathways and cell hierarchies.

Multiplexing is dependent on the ability of an imaging technique to resolve signals from each chemical reporter. For fluorescence microscopy, brightness and areal density of the fluorophore determine intensity of emission. Peak broadening proportional to fluorophore density can produce spectral overlap and potential false-positive measurements. A typical fluorescence

IHC assay uses emission from three sources (*e.g.* two fluorophore-labelled secondary antibodies and a dye such as 4',6-diamidino-2-phenylindole [DAPI], that fluoresces when bound to a specific structural marker, in this case DNA), though some commercial autostainer and microscopy systems have been optimised for up to seven specific fluorophores. Quantum dots (QDs) offer several advantages over traditional fluorophores. Fluorescent emission of QDs is proportional to size, with larger diameter dots emitting into the near-IR region. QDs are resistant to photobleaching and brighter than conventional fluorophores, and surface chemistry can target specific ligands on whole antibodies or antibody fragments, as well as single-chain variant fragment fusion proteins. A detailed overview and protocol for designing multiplexed IHC experiments with QDs can be found in Xing *et al.*<sup>26</sup>

Even greater flexibility is provided by MS for imaging metal-tagged antibodies, which shifts the limiting factor from spectral overlap to the number of unique combinations of primary and secondary antibody host species used for indirect detection (Fig. 5a), or the number of antibodies to which unique photo-cleavable mass tags can be conjugated for molecular mass spectrometry (see below). The true power of elemental MS imaging for multiplexed IHC is evident when applied to direct detection, which is limited only by the number of separate analytes that can be associated with each primary antibody (Fig. 5b). This was demonstrated by Giesen *et al.*,<sup>27</sup> who used commercial MaxPar<sup>®</sup> monoisotopic lanthanide tagging kits to label and simultaneously image 32 antibodies at 1  $\mu\text{m}$  resolution (Fig. 5c) with a laser ablation system coupled to a CyTOF-MS (an ICP-MS design optimised for mass cytometry). This particularly elegant study not only demonstrated a near-five-fold improvement on the maximum number of antigens that can be detected using fluorescence microscopy; it also described an image processing algorithm using lanthanide-labelled structural features to segment and extract data from single cells which subsequently underwent spanning-tree progression analysis of density-normalised events (SPADE) to characterise tumour heterogeneity in breast cancer tissue microarrays. Designed for CyTOF mass cytometry, SPADE examines multidimensional datasets to characterise cell-cell interactions and transitions to construct hierarchical trees of diverse cell populations, it has enormous potential for examining spatial interactions between antigens and associated endogenous chemicals. Angelo *et al.*<sup>28</sup> used a similar IHC protocol with nanoSIMS detection and their own cell-segmentation algorithm to image 10 analytes at 200–300 nm resolution, and used both signal intensity and categorical expression (*i.e.* positive or negative) to build composite images representing immunohistochemical and phenotypic features of malignant cells (Fig. 5d). Both studies used classical light and fluorescence microscopy to demonstrate specificity and sensitivity (Fig. 5e and f). The LA-CyTOF-MS system originally described by Giesen *et al.*<sup>27</sup> was recently commercialised as the Helios<sup>™</sup> by Fluidigm, from which the first applications are now emerging.<sup>29</sup> By design, the Helios<sup>™</sup> system is optimised for high-mass lanthanide detection, thus simultaneous imaging of biologically-relevant elements, most of which fall below the



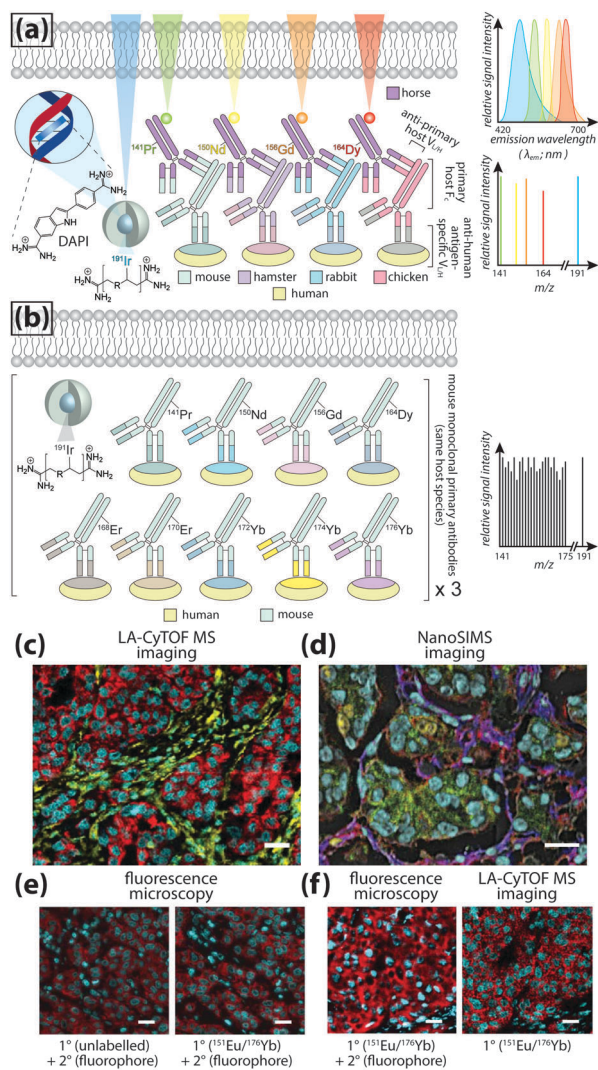


**Fig. 5** Multiplexed IHC using fluorescence microscopy and MS imaging. (a) Simplified conceptual schematic of multiplexed IHC using four secondary antibodies and a DNA-specific probe. Primary antibodies for human antigens raised in four different species are indirectly detected by secondary antibodies with conjugated fluorophores. Resolving signal associated with each antigen requires complex optics and fluorophore emission spectra with minimal overlap. An alternative to overcome spectral overlap uses secondary antibodies labelled with monoisotopic lanthanides (coloured here to match fluorescent tags) and an iridium-containing DNA intercalator, followed by MS imaging. (b) Direct detection of primary antibodies capitalising on the resolving power of MS can be used to substantially increase the number of target antigens. (c) Three-colour LA-CyTOF-MS image of  $^{174}\text{Yb}$ -tagged cytokeratin 8/18 (red),  $^{176}\text{Yb}$ -tagged H3 (cyan) and  $^{162}\text{Dy}$ -tagged vimentin (yellow) from a 32-plexed human breast cancer tissue microarray.<sup>27</sup> (d) Composite nanoSIMS image of mass intensities for cytoplasmic  $^{168}\text{Er}$ -tagged actin (red),  $^{158}\text{Gd}$ -tagged E-cadherin (green) and  $^{154}\text{Sm}$ -tagged vimentin (blue) with nuclei categorically classified as either  $^{139}\text{La}$ -ER $\alpha$  +  $^{145}\text{Nd}$ -PR positive (aqua) or  $^{139}\text{La}$ -ER $\alpha$  +  $^{145}\text{Nd}$ -PR +  $^{150}\text{Nd}$ -Ki67 positive (yellow).<sup>28</sup> (e) Addition of lanthanide tags to primary antibodies ( $^{151}\text{Eu}$ -tagged HER2 [red] and  $^{176}\text{Yb}$ -tagged H3 [cyan]) does not affect binding of fluorophore-conjugated secondary antibodies, and (f) MS imaging reproduces immunofluorescence specificity.<sup>27</sup> Panels (c), (e) and (f) reproduced with permission from Giesen *et al.*,<sup>27</sup> panel (d) reproduced with permission from Angelo *et al.*<sup>28</sup> (both Nature Publishing Group, Copyright 2014).

80 amu threshold, is hardware-limited. New ICP-TOF-MS systems capable of concurrently measuring both low- and high-mass elements, such as the TOFWERK design, will eventually be used for correlative LA-ICP-MS imaging of multiplexed IHC with endogenous metals and heteroatoms.

Photocleavable mass tags can be used in a similar approach for multiplexed IHC experiments using molecular MS imaging, allowing detection of intact proteins normally outside the mass range of TOF mass analysers. Here, the analyte consists of a molecule or peptide with a known mass linked to the antibody *via* an organic linker (either directly or as part of an avidin-biotin complex) with a photo-sensitive region that releases the mass tag when exposed a specific wavelength, normally that of the MALDI ionisation source. By not applying a matrix prior to analysis, signal-to-noise ratios for the applied mass tags allow for highly sensitive targeted multiplexed detection using both primary antibodies<sup>30</sup> and enzyme activity probes.<sup>31</sup> Subsequent matrix application and traditional MALDI-MS imaging can then be used to examine spatial associations between mass-tagged antigens and endogenous biomolecules.

Most examples of IHC-chemical imaging using vibrational spectroscopy take advantage of stimulated Raman scattering, which produces vibrational transitions around 150 times narrower than fluorescence emission spectra. Wei *et al.*<sup>32</sup> synthesised a panel of 14  $\pi$ -conjugated C $\equiv$ C or C $\equiv$ N-containing dyes with isotopic  $^{13}\text{C}$  and  $^{15}\text{N}$  substitution to supplement six commercial Raman-scattering dyes and four fluorophores to simultaneously resolve 24 analytes in multiplexed IHC-stained cultured cells and tissue sections. Functionalisation of antibodies with materials such as gold and silver nanomaterials can be used with surface enhanced Raman scattering (SERS) and surface plasmon resonance spectroscopy for multiplexed imaging, where the size and shape of conjugated particles can be manipulated to produce a unique, resolvable signal.<sup>33</sup>

### 3.3 Validating IHC-chemical imaging experiments

To date, most applications of IHC using chemical imaging have been proof-of-concept and focused primarily on the analytical technique used, as opposed to the full suite of analytical validation steps that would ordinarily be taken for more routine experiments where a known target is isolated, identified, and quantified. Fitzgibbons *et al.*'s Principles of Analytic Validation of Immunohistochemical Assays<sup>11</sup> is required reading when developing any IHC-based chemical imaging experiment. Although the 14 guideline statements are geared toward eventual FDA approval of a new IHC method, they are conceptually analogous to standard validation steps common to analytical chemistry. When setting the rubric, the CAP approached the issue with the overarching question of "[w]hat is needed for initial analytic assay validation before placing any IHC test into clinical service and what are the revalidation requirements?".<sup>11</sup> Rather than dissect the 14 guideline statements, we will examine the five scope questions on which Fitzgibbons *et al.* based their recommendations, and use a hypothetical experiment studying copper metabolism in the mouse brain using LA-ICP-MS (Fig. 6a) to illustrate how analytical validation can be applied to any research-based IHC chemical imaging scenario.



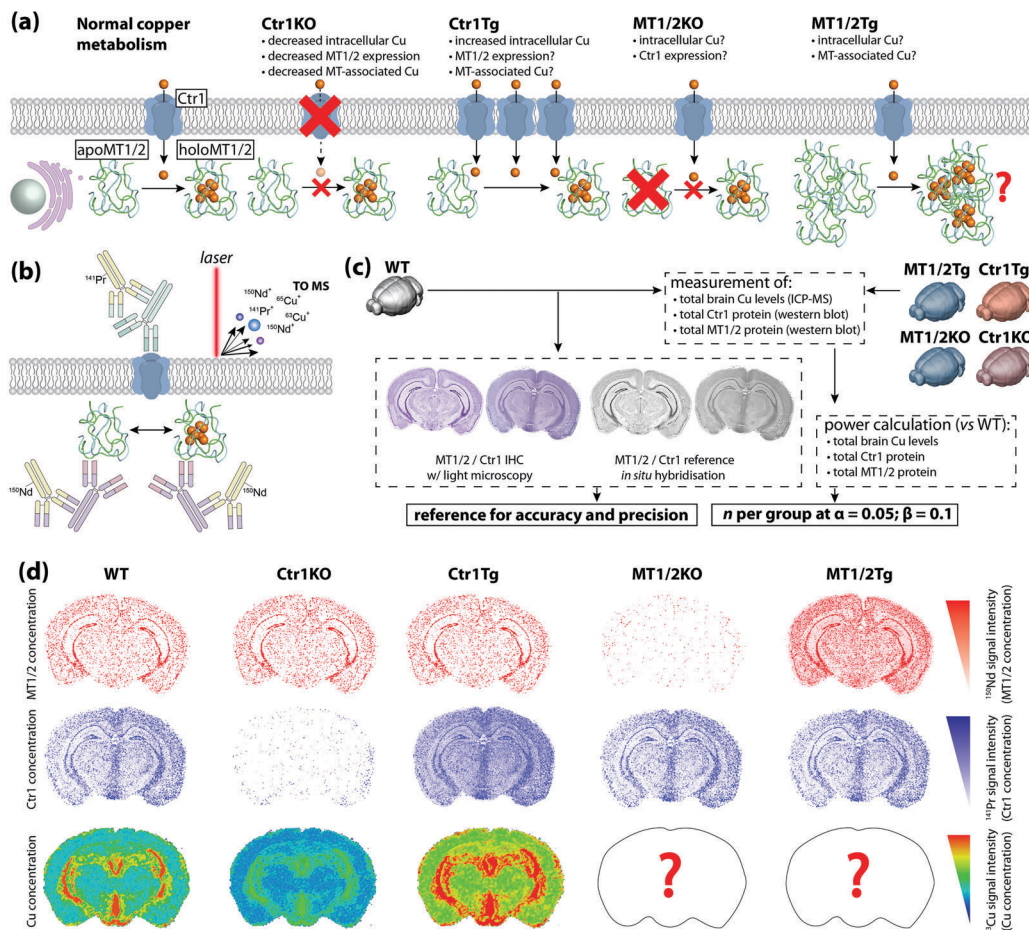


**Fig. 6** Hypothetical experimental design and validation using IHC-chemical imaging. (a) Two major regulators of cellular copper homeostasis are the intramembrane protein copper transporter 1 (Ctr1) and cytosolic metallothionein (MT) family, of which MT1 and 2 isoforms are most abundant. Knock-out (KO) of Ctr1 decreases cellular concentration, whereas transgenic overexpression (Tg) increases copper content. The aim of this hypothetical experiment is to compare Ctr1 modulation with MT1/2 KO and Tg mice with respect to brain copper concentration and distribution. (b) Ctr1 and MT1/2 are detected using modified IHC protocols with lanthanide-tagged secondary antibodies, and distribution of lanthanides and endogenous copper imaging using LA-ICP-MS. (c) Several routine techniques including standard IHC with light microscopy detection, use of reference *in situ* hybridisation databases,<sup>25</sup> total tissue copper assay by ICP-MS, and western blotting for relative protein concentration are used to determine accuracy, precision and sample size. (d) When applied to a fully developed IHC-LA-ICP-MS method, spatial copper distribution in the brain can be compared and contrasted with wild type and Ctr1 KO/Tg animal.

**3.3.1 When and how should validation assess analytic[al] sensitivity, analytic[al] specificity, accuracy (assay concordance), and precision (interrun and interoperator variability)?** The development of a new IHC-chemical imaging method should aim to design, conduct, analyse, interpret, and report protocols in a way that can be independently replicated. In their systematic review of literature conducted to set guidelines for IHC validation, Fitzgibbons *et al.* found only 126 of a total 1463 extracted studies (8.6%) met inclusion criteria,<sup>11</sup> highlighting the lack of consensus regarding an appropriate approach to confirm IHC assay validity.

In our hypothetical experiment, a multiplexed approach using lanthanide-tagged secondary antibodies was developed and applied to image two major copper regulatory proteins, copper transporter-1 (Ctr1) and metallothionein (MT) in sections from fresh-frozen, paraformaldehyde-fixed wild-type and transgenic murine brains using modified IHC protocols, while simultaneously

monitoring how regional copper levels are affected by ablation and overexpression of either protein (Fig. 6b). The animals used were the wild-type background strain (hereafter WT), heterozygous Ctr1 mice (Ctr1KO)<sup>34</sup> and a hypothetical overexpressor (Ctr1Tg; overexpression of Ctr1 and resulting copper accumulation has been demonstrated *in vivo*<sup>34</sup>), combined MT1/2-null (MT1/2KO) and transgenic overexpressors (MT1/2Tg).<sup>35</sup> Analytical sensitivity and specificity were assessed from the outset using antibody titrations and isotype controls to experimentally determine the optimal antibody concentrations.

Two questions regarding specificity can be raised. Firstly, can MT1 be distinguished from MT2, and could cross-reactivity with MT3 produce false-positive data? Most commercial antibodies target N-terminus epitopes in the  $\beta$ -domain that share 100% homology between MT1 and 2; differentiation of MT1 and 2 would require raising monoclonal antibodies specific to one isoform and confirmation by ELISA.<sup>36</sup> Within the context of



this experiment, where MT1 and 2 perform an equivalent function and manipulation of protein expression was universal, differentiation of isoforms was not considered necessary. Regarding MT3, the  $\beta$ -domain epitope shares only three common residues and cross-reactivity is absent<sup>36</sup>—this could be experimentally demonstrated by the presence of MT3 staining in MT1/2KO animals.

The second is whether MT and non-MT copper can be distinguished. In this case, only spatial association between MT1/2 and copper can be inferred from LA-ICP-MS images as the analyte marking MT1/2 spatial distribution is indicative of the protein only, whereas copper images represent all chemical forms in the sample. Thus, appraising the direct relationship between MT1/2 and associated copper levels would require additional biochemical analysis and subsequent loss of spatial information.

Determining accuracy and precision requires a reference standard against which chemical images can be compared (Fig. 6c). Where a relatively low spatial resolution is being used comparisons against light microscopy images may be sufficient, though using a non-IHC assay (*i.e. in situ* hybridisation in either the source material<sup>11</sup> or from open-access databases<sup>25</sup>) increases confidence. The proportional response to concentration adds an additional dimension when assessing precision. Inter-experiment and inter-operator precision is assessed as reproducible localisation of tagged Ctr1 and MT1/2, and a consistent signal intensity in repeated measures of WT animals where relative protein expression levels have been externally confirmed (*i.e.* by western blot). A minimum concordance rate of 90% is the recommended standard for IHC.<sup>11</sup>

**3.3.2 What is the minimum number of positive and negative cases that need to be tested to analytically validate an IHC assay for its intended use(s)?** The expert consensus opinion of Fitzgibbons *et al.*<sup>11</sup> states that non-predictive factors should be validated using 10 positive and 10 negative cases (in this case WT vs. Tg overexpressors and/or KO animals), increasing to 20 for predictive marker (factors with a confirmed association to treatment response or resistance) assays. In our example, copper levels should also be considered; heterozygous Ctr1-null mice (homozygotes display embryonic lethality) exhibit a 50% decrease in total brain copper levels.<sup>34</sup> With such a substantial difference between WT and Ctr1KO animals, a statistical power calculation would suffice with <10 animals per group, though for MT1/2KO mice where effects on brain copper levels are more subtle,<sup>35</sup> a larger experimental population may be required. Power calculations based on quantitative measurement of total copper, Ctr1, and MT1/2 protein expression aid in determining the sufficient number of cases for validation.

**3.3.3 What parameters should be specified for the tissues used in the validation set?** The aim of the hypothetical imaging experiment described was to determine how altering two major copper regulatory proteins influenced regional copper levels and spatial associations. Therefore, the validation set is the experimental group against which others are to be compared. As for any IHC experiment, all possible confounding parameters should be controlled for, beginning with sample collection and

ending with how data is analysed. All samples should undergo identical preparations steps, use single-origin reagents and antibodies, and be analysed using the same LA-ICP-MS system.

**3.3.4 How do certain preanalytic variables influence analytic validation?** Controlling preanalytic variables for IHC-chemical imaging in a research setting such as the example described is relatively simple: animals are sourced from the same background genetic strain, housed in the same conditions (light/dark cycle; water and food from the same source), and tissue prepared using a standard protocol. However, even with consistency across sample preparation methods, there may be differential effects on certain analytical targets. For instance, Ctr1 overexpression may increase cellular copper levels to a point where microchemical equilibria is disrupted so much as to increase labile copper, which is disproportionately lost during fixation and staining, compared to WT where labile copper is essentially absent and protein-copper ligands are resistant to chemical perturbations. While there is no gold standard of native metal spatial distribution against which it can be compared,<sup>37</sup> external measurement of total copper levels in unadulterated tissue, as well as quantitative measurement of copper levels in tissue prior to and after each processing step could be employed to either confirm metal levels are unaffected, or determine the degree of change and whether it is consistent across multiple samples. This can be achieved using LA-ICP-MS imaging, or by independent methods including autoradiography or histochemical stains (reviewed by McRae *et al.*<sup>6</sup>), although in the latter case it should be acknowledged that harsh chemical conditions may perturb native distribution, sensitivity is substantially lower than MS imaging, and precipitation with other endogenous metals may produce false-positives.

**3.3.5 What conditions require assay revalidation?** With all variables controlled and appropriate sample numbers analysed, our hypothetical experiment has reached a point where analytically valid comparisons between groups can be made (Fig. 6d). Further experiments can be carried out using the same experimental conditions, though several scenarios would require some degree of revalidation. Adapting the recommendations by Fitzgibbons *et al.*,<sup>11</sup> new reagents should be tested with one negative and positive control, and minor modifications to the protocol such as incubation time, antibody dilution and batch (assuming the same clone), should be confirmed with two negative and positive control cases. Additional factors to consider include variable antibody-analyte labelling and detection efficiencies between analytical systems. For lanthanide tagging and mass cytometry, Tricot *et al.*<sup>38</sup> identified areas where method standardisation and data normalisation are necessary for interlaboratory harmonisation, all of which are directly relevant to MS imaging and conceptually applicable to other chemical imaging modalities.

## 4. Opportunities and future challenges

Potential applications for IHC-chemical imaging are vast and varied, and primarily depend on two variables: the chemical



nature of the analyte serving as a fiducial proxy for the antigen of interest; and other biomolecules with which they are associated, which may be either endogenous or labelled with different chemical reporter. In the following section, we provide a brief summary of where IHC-chemical imaging can provide new insight into functional biochemistry and discuss the challenges that will arise as the field continues to evolve.

#### 4.1 Multimodal imaging

Multimodal imaging describes the use of different detection techniques used in sequence (asynchronous) or simultaneous collection of signals from multiple analyte classes (synchronous). Both approaches have inherent technical challenges; asynchronous imaging requires registration of sequential images using appropriate fiducial markers, while synchronous imaging often involves complex, multistep sample preparation. Asynchronous imaging should ideally have similar spatial resolution. As an example on the extreme end, super resolution microscopy can achieve spatial resolutions at or below the spatial dimensions of a typical IgG molecule, and identification of a biomolecule is typically achieved through recognition of a specific peptide or amino acid sequence by a small molecule fluorophore attached by either direct conjugation or enzymatic delivery.<sup>39</sup> When coupled with electron microscopy and a common detectable analyte, such as fluorescent tetramethylrhodamine which mediates photooxidation and induces polymerisation of DAB, correlative multimodal images of genetically-encoded tetramethylrhodamine-sensitive proteins and cell ultrastructure can be generated.<sup>40</sup>

Que *et al.*<sup>41</sup> applied a particularly innovative asynchronous multimodal approach using a Zn<sup>2+</sup>-sensitive fluorescent sensor and live-cell imaging (Fig. 7a) with subsequent scanning transmission electron microscopy with energy-dispersive spectroscopy, and synchrotron-based XFM and three-dimensional elemental tomography to characterise zinc flux during oocyte maturation. This method demonstrated that multimodal imaging need not necessarily be performed on the same sample; information gleaned from one technique was built upon by unique capabilities of following imaging modalities to quantitatively assess how 'zinc sparks' necessary for transition from egg-to-embryo form and change subcellular compartmentalisation.

Capabilities of diffraction-limited fluorescence microscopy are constantly being expanded by application of fluorophores with greater quantum yields, and the development of novel fluorescent sensors for endogenous chemicals, recently reviewed by Kolanowski *et al.*<sup>43</sup> Synchronous fluorescence microscopy combining IHC with inducible fluorescence in transfected cell lines, organelle markers, and small molecule sensors have produced subcellular images with remarkable levels of detail (Fig. 7b).

#### 4.2 Small molecule sensors and temporal imaging

Over the last several decades a catalogue of cell-permeable and highly-specific compounds that fluoresce in the presence of small molecules have become commercially available, and the synthesis of novel chemical sensors is a vibrant field of research.<sup>44</sup>

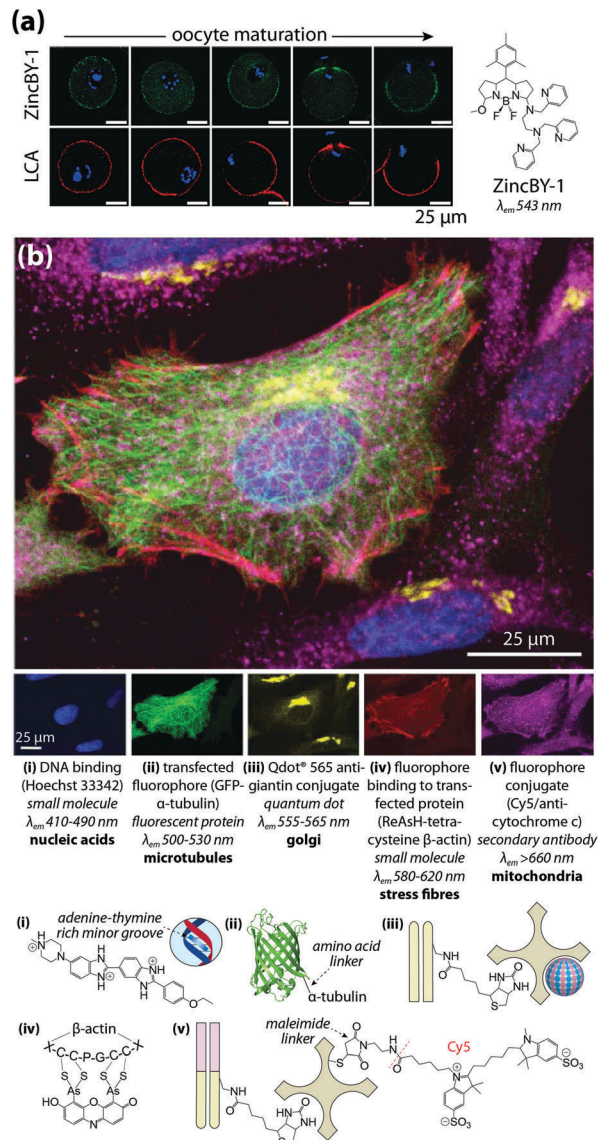


Fig. 7 Asynchronous and synchronous multimodal imaging (a) sequential fluorescence imaging of 'zinc sparks' in maturing mammalian oocytes. Murine cells at five distinct stages of meiosis were labelled with the Zn<sup>2+</sup> sensor ZincBY-1 (green) and counterstained with a DNA-binding fluorophore (blue). Oocytes were then fixed with paraformaldehyde and stained with fluorescent *Lens culinaris* agglutinin (LCA; red) and nucleic acid-marker DAPI (blue). LCA selectively binds to lectins on the surface of cortical granules, and the similar pattern of ZincBY-1 fluorescence suggests these vesicles are laden with Zn<sup>2+</sup>. Combined with XFM imaging, this method was able to quantify the total zinc content of a single oocyte (6 × 10<sup>10</sup> atoms). Reproduced with permission from Que *et al.* (Nature Publishing Group, Copyright 2014).<sup>41</sup> (b) Merged (top) and false-colour (bottom panels) images of parallel microscopy of HeLa cell structural features using five distinct fluorescent analytes: (i) bisbenzimidazole (Hoechst 33342) binding to adenine–thymine-rich DNA minor grooves; (ii) transfection and expression of green fluorescent protein (GFP) bound to  $\alpha$ -tubulin via a six-amino acid linker; (iii) secondary antibodies with quantum dot conjugates; (iv) 4',5'-bis(arsenoso)resorufin (ReAsH) binding to mutant  $\beta$ -actin containing a tetracysteine (Cys-Cys-Pro-Gly-Cys-Cys) motif; and (v) traditional ICH with a Cy5–streptavidin–biotin fluorophore bound to the Fab region of a secondary IgG antibody. Reproduced with permission from Giepmans *et al.* (American Association for the Advancement of Science, Copyright 2006).<sup>42</sup>





Fluorophores specific to by-products of cellular respiration (such as reactive nitrogen, oxygen, and sulfur species) at nanomolar levels have provided new insight into cellular redox state and subcellular effects of oxidative stress, and can be multiplexed to spatially profile biochemical interactions.<sup>43</sup> Specificity to a particular redox state permits snapshots of dynamic biochemical equilibria, and reversible probes with stable quantum yields over multiple redox cycles can be used to temporally profile changes to cellular oxidative state as a result of normal cellular function or chemical stimuli used as a disease mimetic. While these probes can theoretically be coupled with antibody-conjugated fluorophores in permeabilised cells, unavoidable perturbations to native cellular redox state arising from IHC protocols limits applications in live cell imaging.

### 4.3 Intact systems

Several methods for optical clearing, such as 3DISCO and CLARITY, are allowing interrogation of structural and molecular networks in intact biological systems using three-dimensional microscopy such as confocal and light-sheet methods. CLARITY is particularly appealing as impregnation of tissue with a fixative and hydrogel monomer forms a polymerised ‘mesh’ support to which proteins are bound.<sup>45</sup> Addition of sodium dodecyl sulfate then allows electrophoretic clearing of optically-opaque lipids, leaving a transparent sample amenable to repeated IHC staining, imaging, and antibody clearing using a detergent. Sequential staining cycles produce diminishing returns, as approximately 8% of hydrogel-anchored proteins are lost during each surfactant clearing step. The ideal scenario for CLARITY would be single clearing step followed by multiplexed IHC with several fluorophores covering a pre-determined panel of target biomolecules. Superior optical properties of QDs would appear to be best suited, though QD-conjugated antibodies are unable to match traditional fluorophores with respect to tissue penetration depth. Nevertheless, CLARITY and associated methods are relatively new tools that will undoubtedly improve over the coming years.

### 4.4 *In situ* quantification

Traditional IHC assesses sensitivity and quantification in a somewhat arbitrary and subjective manner based on visual inspection of sections using light microscopy. A pathologist may assign a binary positive/negative score with reference to a positive control, use a narrow numerical range to rank staining intensity (*i.e.* 1–4), or apply other grading systems that assess both staining intensity and percentage of positive cells (*e.g.* H-scoring, quick scoring or the Allred method<sup>46</sup>). Each method is manual, prone to inter-observer bias, and chromogen development is difficult to standardise. Recent advances in digital image analysis, such as the IHC Profiler plugin for ImageJ automate spectral deconvolution of 3,3'-diaminobenzidine (DAB)-enhanced IHC-labelled cancer biopsies to segment and score staining intensity on a pixel-by-pixel basis, reducing observer bias,<sup>47</sup> though the resultant 8-bit colour image is still used to stratify data according to four-point grading. The availability of more comprehensive image analysis algorithms for ImageJ, such as those in the Fiji (Fiji Is Just ImageJ) package,<sup>48</sup>

have dramatically expanded the capabilities of this public-domain resource, and are applicable to all imaging modalities. Additionally, by making algorithms used for cell segmentation and data analysis, such as that used by Giesen *et al.*,<sup>27</sup> publicly accessible and in either open-access or commonly-used proprietary programming languages, templates for custom-designed image analysis software suited to the method used are available.

Absolute quantification of an antigen using chemical imaging is, at least in theory, achievable, though considering the multiple variables in existing IHC protocols that necessitate re-validation it is unlikely that reproducible *in situ* quantification would ever become mainstream. The ‘antibody binding capacity’, or ABC, of a sample can be determined according to the following:<sup>49</sup>

$$ABC = n_1\theta_1\lambda_1 \quad (1)$$

where  $n_1$  represents the number of antigen-binding sites,  $\theta_1$  is the fraction of antigens to which a primary antibody is bound, and  $\lambda_1$  is the valence of the primary antibody (*i.e.*  $\lambda_1 = 0.5$  for a primary antibody where both paratopes recognise antigens on two molecules). Two factors further contribute to the ABC of a cell: steric hindrance of the epitope and non-specific binding. McCloskey *et al.*<sup>50</sup> extended the ABC concept to determine  $\Psi$ , which uses the same parameters to quantify recognition of the primary antibody by indirect detection:

$$\Psi = n_2\theta_2\lambda_2 \quad (2)$$

Thus, if such an approach were to be applied to IHC-chemical imaging, foreknowledge of antigen–antibody binding characteristics, which vary substantially between batches and clones, would be needed. Additionally, the number of antigen binding sites ( $n$ ) would have to be determined by an external method, such as quantitative liquid chromatography-MS/MS for each sample, after which the value of spatially assessing concentration may become moot. External calibration could be applied, where known concentrations of the target antigen are deposited on a suitable substrate and undergo IHC preparation in parallel, though this depends on: (i) the availability of purified protein standards; (ii) complete characterisation of antibody binding efficiency to give  $\theta$  and  $\lambda$ ; and (iii) confidence that the substrate on which the standard is deposited is equivalent to the sample. This latter point presents the biggest challenge; the factors influencing  $\theta$  are all related to the presence of the antigen in a complex cellular environment, one which cannot be easily replicated using standard reference materials. There is no doubt that novel methods for *in situ* quantification will be developed in the future, though these will likely be application-specific, and current methods were relative comparisons or categorical classifications are used will continue to prevail.

## 5. Conclusions

Integrating IHC with chemical imaging represents the forefront of transdisciplinary chemistry. As outlined in this Tutorial Review, designing, executing, and validating an imaging experiment using antibodies and novel analytes requires knowledge



spanning the fundamental principles of IHC to the technical intricacies of advanced analytical methods. However, with a sound and methodical approach to conducting IHC-chemical imaging experiments, the potential insight into complex biochemical processes that stands to be gained is, metaphorically speaking, almost immeasurable.

## Conflicts of interest

P. A. D. and D. J. H. receive research and material support from Agilent Technologies and ESI Ltd through the Australian Research Council Linkage Projects scheme. D. J. H. also receives research and material support from Agilent Technologies through the National Health and Medical Research Council Career Development Fellowship (Industry) program.

## Acknowledgements

DPB is supported by an Australian Research Council Discovery Early Career Researcher Award (DE180100194). PAD is the recipient of an Australian Research Council Discovery Project (DP170100036). TZ is supported by a Parkinson's Victoria PhD Scholarship. DJH is supported by an Australian National Health and Medical Research Council Industry Career Development Fellowship (1122981) in partnership with Agilent Technologies. Due to space limitations, this Tutorial Review could not give appropriate credit to all research in this field, and we wish to acknowledge to the authors of the many great works that were not cited directly.

## References

- 1 A. Coons, H. Creech and R. Jones, *Exp. Biol. Med.*, 1941, **47**, 200–202.
- 2 K. Thorn, *Mol. Biol. Cell*, 2016, **27**, 219–222.
- 3 U. Kubitscheck, *Fluorescence Microscopy: From Principles to Biological Applications*, John Wiley & Sons, 2nd edn, 2017.
- 4 N. Vogler, S. Heuke, T. W. Bocklitz, M. Schmitt and J. Popp, *Annu. Rev. Anal. Chem.*, 2015, **8**, 1–29.
- 5 R. Fernandez-Leiro and S. H. W. Scheres, *Nature*, 2016, **537**, 339–346.
- 6 R. McRae, P. Bagchi, S. Sumalekshmy and C. J. Fahrni, *Chem. Rev.*, 2009, **109**, 4780–4827.
- 7 J. M. Pushie, I. J. Pickering, M. Korbas, M. J. Hackett and G. N. George, *Chem. Rev.*, 2014, **114**, 8499–8541.
- 8 J. Kaiser, K. Novotný, M. Z. Martin, A. Hrdlička, R. Malina, M. Hartl, V. Adam and R. Kizek, *Surf. Sci. Rep.*, 2012, **67**, 233–243.
- 9 A. Bodzon-Kulakowska and P. Suder, *Mass Spectrom. Rev.*, 2016, **35**, 147–169.
- 10 A. R. Buchberger, K. DeLaney, J. Johnson and L. Li, *Anal. Chem.*, 2017, **90**, 240–265.
- 11 P. L. Fitzgibbons, L. A. Bradley, L. A. Fatheree, R. Alsabeh, R. S. Fulton, J. D. Goldsmith, T. S. Haas, R. G. Karabakhtsian, P. A. Loykasek, M. J. Marolt, S. S. Shen, A. T. Smith and P. E. Swanson, *Arch. Pathol. Lab. Med.*, 2014, **138**, 1432–1443.
- 12 K. Dreisewerd, *Chem. Rev.*, 2003, **103**, 395–426.
- 13 Y. Chen, J. Cai, Q. Xu and Z. W. Chen, *Mol. Immunol.*, 2004, **41**, 1247–1252.
- 14 D. J. Hare, E. J. New, M. D. de Jonge and G. McColl, *Chem. Soc. Rev.*, 2015, **44**, 5941–5958.
- 15 W. F. Wolkers and H. Oldenhof, *Cryopreservation and Freeze-Drying Protocols*, Springer-Verlag, New York, 2015.
- 16 A. G. Bittermann, G. Knoll, A. Németh and H. Plattner, *Histochemistry*, 1992, **97**, 421–429.
- 17 M. J. Hackett, J. A. McQuillan, F. El-Assaad, J. B. Aitken, A. Levina, D. D. Cohen, R. Siegele, E. A. Carter, G. E. Grau, N. H. Hunt and P. A. Lay, *Analyst*, 2011, **136**, 2941–2952.
- 18 A. J. Hobro and N. I. Smith, *Vib. Spectrosc.*, 2017, **91**, 31–45.
- 19 J. Chwiej, M. Szczerbawska-Boruchowska, M. Lankosz, S. Wojcik, G. Falkenberg, Z. Stegowski and Z. Setkiewicz, *Spectrochim. Acta, Part B*, 2005, **60**, 1531–1537.
- 20 D. J. Hare, J. L. George, L. Bray, I. Volitakis, A. Vais, T. M. Ryan, R. A. Cherny, A. I. Bush, C. L. Masters, P. A. Adlard, P. A. Doble and D. I. Finkelstein, *J. Anal. At. Spectrom.*, 2013, **29**, 565–570.
- 21 A. W. Foster, D. Osman and N. J. Robinson, *J. Biol. Chem.*, 2014, **289**, 28095–28103.
- 22 P. B. Bass, K. B. Engel, S. R. Greytak and H. M. Moore, *Arch. Pathol. Lab. Med.*, 2014, **138**, 1520–1530.
- 23 J. A. Ramos-Vara, J. D. Webster, D. DuSold and M. A. Miller, *Vet. Pathol.*, 2014, **51**, 102–109.
- 24 S. R. Shi, M. E. Key and K. L. Kalra, *J. Histochem. Cytochem.*, 1991, **39**, 741–748.
- 25 E. S. Lein, M. J. Hawrylycz, N. Ao, M. Ayres, A. Bensinger, A. Bernard, A. F. Boe, M. S. Boguski, K. S. Brockway, E. J. Byrnes, L. Chen, L. Chen, T.-M. Chen, M. Chin, J. Chong, B. E. Crook, A. Czaplinska, C. N. Dang, S. Datta, N. R. Dee, A. L. Desaki, T. Desta, E. Diep, T. A. Dolbeare, M. J. Donelan, H.-W. Dong, J. G. Dougherty, B. J. Duncan, A. J. Ebbert, G. Eichele, L. K. Estin, C. Faber, B. A. Facer, R. Fields, S. R. Fischer, T. P. Fliss, C. Frensley, S. N. Gates, K. J. Glattfelder, K. R. Halverson, M. R. Hart, J. G. Hohmann, M. P. Howell, D. P. Jeung, R. A. Johnson, P. T. Karr, R. Kawal, J. M. Kidney, R. H. Knapik, C. L. Kuan, J. H. Lake, A. R. Laramee, K. D. Larsen, C. Lau, T. A. Lemon, A. J. Liang, Y. Liu, L. T. Luong, J. Michaels, J. J. Morgan, R. J. Morgan, M. T. Mortrud, N. F. Mosqueda, L. L. Ng, R. Ng, G. J. Orta, C. C. Overly, T. H. Pak, S. E. Parry, S. D. Pathak, O. C. Pearson, R. B. Puchalski, Z. L. Riley, H. R. Rockett, S. A. Rowland, J. J. Royall, M. J. Ruiz, N. R. Sarno, K. Schaffnit, N. V. Shapovalova, T. Svisay, C. R. Slaughterbeck, S. C. Smith, K. A. Smith, B. I. Smith, A. J. Sodt, N. N. Stewart, K.-R. Stumpf, S. M. Sunkin, M. Sutram, A. Tam, C. D. Teemer, C. Thaller, C. L. Thompson, L. R. Varnam, A. Visel, R. M. Whitlock, P. E. Wohnoutka, C. K. Wolkey, V. Y. Wong, M. Wood, M. B. Yaylaoglu, R. C. Young, B. L. Youngstrom, X. Yuan, B. Zhang, T. A. Zwingman and A. R. Jones, *Nature*, 2007, **445**, 168–176.
- 26 Y. Xing, Q. Chaudry, C. Shen, K. Kong, H. E. Zhou, L. W. Chung, J. A. Petros, R. M. O'Regan, M. V. Yezhelyev, J. W. Simons, M. D. Wang and S. Nie, *Nat. Protoc.*, 2007, **2**, 1152–1165.



- 27 C. Giesen, H. A. O. Wang, D. Schapiro, N. Zivanovic, A. Jacobs, B. Hattendorf, P. J. Schüffler, D. Grolimund, J. M. Buhmann, S. Brandt, Z. Varga, P. J. Wild, D. Günther and B. Bodenmiller, *Nat. Methods*, 2014, **11**, 417–422.
- 28 M. Angelo, S. C. Bendall, R. Finck, M. B. Hale, C. Hitzman, A. D. Borowsky, R. M. Levenson, J. B. Lowe, S. D. Liu, S. Zhao, Y. Natkunam and G. P. Nolan, *Nat. Med.*, 2014, **20**, 436–442.
- 29 D. Schulz, V. Zanotelli, J. Fischer, D. Schapiro, S. Engler, X.-K. Lun, H. Jackson and B. Bodenmiller, *Cell Syst.*, 2018, **6**, 25–36.
- 30 G. Thiery, M. S. Shchepinov, E. M. Southern, A. Audebourg, V. Audard, B. Terris and L. G. Gut, *Rapid Commun. Mass Spectrom.*, 2007, **21**, 823–829.
- 31 J. Yang, P. Chaurand, J. L. Norris, N. A. Porter and R. M. Caprioli, *Anal. Chem.*, 2012, **84**, 3689–3695.
- 32 L. Wei, Z. Chen, L. Shi, R. Long, A. V. Anzalone, L. Zhang, F. Hu, R. Yuste, V. W. Cornish and W. Min, *Nature*, 2017, **544**, 465–470.
- 33 H. Xu, Q. Li, L. Wang, Y. He, J. Shi, B. Tang and C. Fan, *Chem. Soc. Rev.*, 2014, **43**, 2650–2661.
- 34 J. Lee, M. J. Petris and D. J. Thiele, *J. Biol. Chem.*, 2002, **277**, 40253–40259.
- 35 S.-i. Ono, D. J. Koropatnick and M. G. Cherian, *Toxicology*, 1997, **124**, 1–10.
- 36 G. Emri, E. Emri, L. Beke, G. Boros, C. Hegedűs, E. Janka, E. Gellén, G. Méhes and É. Remenyik, *J. Met. Nano*, 2015, **3**, 33–42.
- 37 E. J. New, V. C. Wimmer and D. J. Hare, *Cell Chem. Biol.*, 2018, **25**, 7–18.
- 38 S. Tricot, M. Meyrand, C. Sammiceli, J. Elhmouzi-Younes, A. Corneau, S. Bertholet, M. Malissen, R. Grand, S. Nuti, H. Luche and A. Cosma, *Cytometry, Part A*, 2015, **87**, 357–368.
- 39 M. Fernández-Suárez and A. Y. Ting, *Nat. Rev. Mol. Cell Biol.*, 2008, **9**, 929–943.
- 40 V. Liss, B. Barlag, M. Nietschke and M. Hensel, *Sci. Rep.*, 2015, **5**, 17740.
- 41 E. L. Que, R. Bleher, F. E. Duncan, B. Y. Kong, S. C. Gleber, S. Vogt, S. Chen, S. A. Garwin, A. R. Bayer, V. P. Dravid, T. K. Woodruff and T. V. O'Halloran, *Nat. Chem.*, 2014, **7**, 130–139.
- 42 B. N. G. Giepmans, S. R. Adams, M. H. Ellisman and R. Y. Tsien, *Science*, 2006, **312**, 217–224.
- 43 J. L. Kolanowski, F. Liu and E. J. New, *Chem. Soc. Rev.*, 2018, **47**, 195–208.
- 44 E. J. New, *ACS Sens.*, 2016, **1**, 328–333.
- 45 K. Chung, J. Wallace, S.-Y. Kim, S. Kalyanasundaram, A. S. Andalman, T. J. Davidson, J. J. Mirzabekov, K. A. Zalocusky, J. Mattis, A. K. Denisin, S. Pak, H. Bernstein, C. Ramakrishnan, L. Grosenick, V. Gradinaru and K. Deisseroth, *Nature*, 2013, **497**, 332–337.
- 46 D. C. Allred, J. M. Harvey, M. Berardo and G. M. Clark, *Mod. Pathol.*, 1998, **11**, 155–168.
- 47 F. Varghese, A. B. Bukhari, R. Malhotra and A. De, *PLoS One*, 2014, **9**, e96801.
- 48 J. Schindelin, I. Arganda-Carreras, E. Frise, V. Kaynig, M. Longair, T. Pietzsch, S. Preibisch, C. Rueden, S. Saalfeld, B. Schmid, J.-Y. Tinevez, D. White, V. Hartenstein, K. Eliceiri, P. Tomancak and A. Cardona, *Nat. Methods*, 2012, **9**, 676–682.
- 49 R. J. Zagursky, D. Sharp, K. A. Solomon and A. Schwartz, *Biotechniques*, 1995, **18**, 504–509.
- 50 K. E. McCloskey, K. Comella, J. J. Chalmers, S. Margel and M. Zborowski, *Biotechnol. Bioeng.*, 2001, **75**, 642–655.

